Synthesis, NMR, FT-IR, FT-Raman spectra and thermal studies of Choline bis(trifluoromethylsulfonyl)imide ionic liquid combined with DFT calculations

Boumediene Haddad, Silvia Antonia Brandán, María Castillo, Aya Khadidja Touil, Annalisa Paolone, Bekhaled Fetouhi, Nathalie Bar, Didier Villemin, Mustapha Rahmouni, Serge Bresson

Synthesis, NMR, FT-IR, FT-Raman spectra and thermal studies of Choline bis(trifluoromethylsulfonyl)imide Ionic Liquid combined with DFT Calculations.

Boumediene Haddad[1,2,*], Silvia Antonia Brandán[3],María V. Castillo[3], Touil Aya Khadidja[1,4], Annalisa Paolone[5], Bekhaled Fetouhi[6,7],Nathalie Bar[2],Didier Villemin[2], Mustapha Rahmouni[7], Serge Bresson[8]

[1]Department of Chemistry, Faculty of Sciences, University of Saida - Dr. Moulay-Tahar, 20000, Algeria.
[2] LCMT, ENSICAEN, UMR 6507 CNRS, University of Caen, 6 bd MlJuin, 14050 Caen, France
[3]Cátedra de Química General, Instituto de Química Inorgánica, Facultad de Bioquímica. Química y Farmacia, Universidad Nacional de Tucumán, Ayacucho 471, (4000) San Miguel de Tucumán, Tucumán, Argentina
[4]Chemistry Laboratory of Synthesis, Properties, and Applications (CLSPA-Saida), University of Saida, Algeria
[5]CNR-ISC, U.O.S. La Sapienza, Piazzale A. Moro 5, 00185 Roma, Italy
[6]Faculty of Natural and Life Sciences, University of Tiaret, BP78 ZaarouraTiaret 14000, Algeria
[7] Synthesis and Catalysis Laboratory LSCT, Tiaret University, Tiaret, Algeria
[8]UP Transformations & Agro-Ressources, Institut Polytechnique UniLaSalle, SFR Condorcet 3417, BP 30313, F-60026 Beauvais, France.

*Corresponding author: Tel.: +213676802567
E-mail :haddadboumediene@yahoo.com (HADDAD Boumediene).

Abstract

In an environmentally friendly manner, the reaction of choline chloride ([$CHOL^+$][(Cl^-]) with lithium bis(trifluoromethanesulfonyl)imide ([Li^+][($CF_3SO_2)_2N^-$]) in water leads to the formation of the ionic liquid (IL) choline bis(trifluoromethanesulfonyl)imide ([$CHOL^+$][($CF_3SO_2)_2N^-$]).The ionic liquid IL have been characterized by using ^1H, ^{13}C and, ^{19}F-NMR, FT-IR and FT-Raman spectroscopies. The experimental spectra have been combined with B3LYP/6-311++G** calculations to obtain complete assignments of vibrational spectra of IL and its cation by using the scaled mechanical quantum force field (SQMFF) methodology and the Molvib program. Here, we reported the 102 vibration modes of IL and the 36 of cation together with the scaled force constants for both species. The predicted structure shows the formation of the S-O···H interaction in agreement with experiments. Very good correlations evidence the comparisons among the experimental and theoretical NMR, FT-IR and FT-Raman spectra. The existence ofthe strong S-O···H interaction and other weak H bonds interactions are supported by NBO and AIM calculations. The analyses of gap values suggest a higher reactivity of IL in gas phase and a higher stability in aqueous solution. The comparison of this IL with [C_8DABCO^+][($CF_3SO_2)_2N^-$] reveal that the [C_8DABCO^+] cation increases the reactivity of latter IL in solution.Besides a detailed characterization of its thermal (TGA/DSC) is presented. Investigation of the thermal properties demonstrated that the investigated IL can be classified as an ionic liquid, as the melting temperature is near room temperature. A glass transition and a cold crystallization were revealed at -75 and -26 °C.

KEYWORDS: Choline-ionic liquids; bis(trifluoromethylsulfonyl)imide, NMR; Raman/IR vibrational spectra; TGA /DTA thermal analysis; DFT calculations.

1. Introduction

For several years, there has been a increasing concern in the development of new solvents, in particular ionic liquids (ILs) and deep eutectic solvents (DES) [1] meeting certain green chemistry criteria and considering as potential environmentally friendly alternative solvents [2]. Both categories of solvents present attractive characteristics since they have a negligible saturated vapor pressure, are non-flammable and have good thermal and chemical stability [3].These solvents can have very good ionic conduction when ionic molecules are integrated into the mixture [4] opening the possibility of using them in energy-related fields. In addition, the specific properties of ILs, modulated by the appropriate choice of couple anion–cation [5], justify their use in many fields such as the chemical industry [6], medicine [7], nanotechnologies [8], the field of energy [9] and in particular electrochemistry [10] or even in renewable energies [11]. Now, most of researchers have been focusing their attention on the synthesis of new DES and in the study of their properties for device applications. Thus, choline derivatives have been the subjects of numerous studies and play an essential role in the evolution of green chemistry. Therefore, the quaternary ammonium salt choline, also know as hepacholine, biocolina and lipotril and cholonium, has shown interesting and unique physico-chemical properties in various processes extraction [12]. Some metal-free choline-based ionic liquids (ILs) were developed by Liu et al [13], with the aim to use them as catalysts in the glycolysis of PET. Rabhi et al. [14] evaluated a choline bis(trifluoromethylsulfonyl)imide based ionic liquid for the extraction of o-xylene, o-cresol and acetonitrile from the aqueous solution showing a good potential. Domanska et al. [15] found that ($[CHOL^+][(CF_3SO_2)_2N^-]$) strongly interact with pyridene, leading to high heptane/pyridine selectivity, while Cesari et al. [16] demonstrated that $[CHOL^+][(CF_3SO_2)_2N^-]$ is an appropriate solvent to recover phenolic compounds from water. Ribeiro et al. [17] haveinvestigated choline oxyanions salts attached with the acetate and dihydrogen phosphate anions by using the IR and Raman spectra. These authors evidenced the spectral marks of the H-bonds interactions and intramolecular motions of the ions. In other study, Ludwig et al. have revealed the effect of structural and dynamical behaviour of $[CHOL^+][(CF_3SO_2)_2N^-]$ on melting temperatures, viscosities and conductivities[18]. Nockemann et al. [19] reported binary mixtures of water with temperature effect on the thermophysical, and thermomorphic properties, as well as the optical properties of choline bis(trifluoromethanesulfonyl)imide, while Zhuravlev et al. [20] studied the electronic and vibrational properties of ILs synthesized with choline halides. To date, the experimental structure of $[CHOL^+][(CF_3SO_2)_2N^-]$ was determined by Nockemann et al. [19] by XRD but there are no studies reported on

topological, electronic and vibrational properties of[$CHOL^+$][$(CF_3SO_2)_2N^-$] nor any detailled assignments of its vibrational spectra. Hence, the present works aims to synthesize the [$CHOL^+$][$(CF_3SO_2)_2N^-$]IL through a simple metathesis reaction, and to characterize it by using ^1H, ^{13}C and ^{19}F-NMR, infrared, Raman spectroscopy combined with computational techniques in order to perform the complete vibrational assignments. Hence, its scaled harmonic force constants are reported. Moreover, the physical properties were investigated by DSC and TGA while the inter- and intra-molecular interactions are analyzed utilizing natural bond orbital (NBO) and atoms in molecules (AIM) calculations in addition to the IR and Raman spectra. Reactivities and behaviours of IL in different media are also predicted.

2. Experimental

2.1. Materials and methods

In the current work, all materials used had analytical grades and were not purified before being utilized. Choline chloride ([$CHOL^+$][$(Cl^-$]) (purity: 98%), and lithium bis(trifluoromethanesulfonyl)imide ([Li^+][$(CF_3SO_2)_2N^-$]) were commercially available from Fluka. Deionized H_2O was obtained by means of a Millipore ion-exchange resin deionizer.

Choline bis(trifluoromethanesulfonyl)imide, ([$CHOL^+$][$(CF_3SO_2)_2N^-$]) was synthesized at the LCMT *Molecular and Thio-organic Chemistry Laboratory*. Ionic liquid of ([$CHOL^+$][$(CF_3SO_2)_2N^-$]) is prepared following our previous works [21-23], and was characterized by intermediary of NMR, IR and Raman spectroscopy. Firstly, the NMR analysis include^{1}H-NMR (600 MHz), ^{13}C-NMR (150.87 MHz) decoupled only from ^{1}H and^{19}F.^{19}F-NMR (564.04 MHz) spectra were acquired on a Bruker-Neo 600MHz instrument;the chemical shifts were referenced to TMS as external standard. The spectra were measured in dimethylsulfoxide (DMSO-d_6), and the DMSO residual peak was used as the ^{1}H internal reference (quintuplet δ = 2.5 ppm), while the DMSO-$d_6$central peak at δ = 39.5ppm was used as the ^{13}C reference. The Raman spectrum of ([$CHOL^+$][$(CF_3SO_2)_2N^-$]) was acquired by a Vertex 70-RAM II Bruker FT-Raman spectrometer in the4000-45 cm^{-1} range (resolution=1 cm^{-1}, 128 scans for each spectrum) at room temperature. The FT-IR spectrum of ([$CHOL^+$][$(CF_3SO_2)_2N^-$]) was recorded by on a Bruker Vertex II-70RAM Spectrometer between 600and 4000 cm^{-1} (resolution= 1 cm^{-1}, 64 scans per spectrum).

The thermal stability of ([$CHOL^+$][$(CF_3SO_2)_2N^-$]) was examined by thermogravimetric analysis (TGA) between 25and700 °C, while the phase transition were examined by differential scanning calorimeter (DSC) between -80 and 200 °C.A Mettler Toledo DSC3 and a Setaram Setsys Evolution 1200 TGA system were used for DSC and TGA measurements,

which were both performed in an inert (argon) helium flux of 60 mL/min. The temperature rate for the measurements were 5 (DSC) or 10 °C/min (TGA).

In the present study, the choline bis(trifluoromethanesulfonyl)imide ($[CHOL^+][(CF_3SO_2)_2N^-]$) was synthesized through a simple anion exchange reactions as shown in **Scheme 1**.A solution of2.87g(0.1M) of lithium bis(trifluoromethylsulfonyl)imide ($[Li^+][(CF_3SO_2)_2N^-]$) in 15 mL of distilled water and a solution of 1.32g (0.1M) of Choline chloride ($[CHOL^+][(Cl^-]$) in 15 mL of distilled water were mixed in a flask with stirring for 1 hour at room temperature. After isolation of ($[CHOL^+][(CF_3SO_2)_2N^-]$) (bottom) from lithium chloride (top) by centrifugation for 60 sinthe aqueous phase, the obtained ($[CHOL^+][(CF_3SO_2)_2N^-]$)was washed a few times by deionized water in order to remove chloride impuritiesandthen dried in a vacuum better then 1 mbar for 12 h, to obtain a colorless liquid. Finally,($[CHOL^+][(CF_3SO_2)_2N^-]$) was dried in Ca_2Cl_2 to remove water traces. Coulometric Karl Fischer titration, performed by a Metrohm 831 instrument, found a water content lower than 523 ppm.

Scheme 1. Generalsynthesis of Choline bis(trifluoromethylsulfonyl)imide.

2.2. Computational details

The starting initial structures of $[CHOL^+][(CF_3SO_2)_2N^-]$ IL and its cation were extracted from the CIF file of Ref [19] while the anion was removed from the IL using *GaussView*[26]. The structures of the cation and of the IL were optimized both in vacuum and in an aqueous solution at the B3LYP/6-311++G** level of theory/basis set, by means of Gaussian 16 [24,25,27].The structure of $[(CF_3SO_2)_2N^-]$ anion was taken from that previously reported at the same level of theory [21,22]. The integral equation-formalism polarizable continuum model (IEF-PCM) and universal solvation method (SMD) calculations were used for all calculations in solution [28-30].The MOLDRAW program was applied for the volume calculations [31].A calculation of the vibration frequencies was performed for all optimized structures.

The NBO and AIM2000 programs were employed to calculate atomic charges, bond orders stabilization energies, and topological properties [32-35]. The reactivity of the species was calculated based on frontier orbitals [21,22,36-37]. Harmonic force fields of the species were calculated and the assignment of the vibrations was performed accordingly. For that purpose, the scaled quantum mechanical force field (SQMFF) methodology was employed using

MOLVIB [38-40].The Raman spectra predicted for the three specie in activities were transformed to intensities [41]. The electronic spectra in aqueous solution were investigated using time-dependent DFT calculations (TD-DFT) performed by Gaussian 16 [24,25,27].program by [26]. The NMR spectra were calculated applying the Gauge-Independent Atomic Orbital (GIAO) method [42].

3. Results and discussion

3.1. NMR spectra analysis

The synthesized [$CHOL^+$][$(CF_3SO_2)_2N^-$] IL was characterized by using ^1H, ^{13}C and ^{19}F-NMR spectroscopy technique. The experimental ^1H, ^{13}C and and^{19}F-NMR are given respectively in **Figs. 1, 2 and 3**. The NMR spectra show the following signals. **^{1}H-NMR** (600 MHz, DMSO-d_6) δ_H(ppm): 3.10 (s,CH_3, 9H), 3.40 (t, NCH_2, 2H, J=1.8 Hz),3.83 (tt, CH_2, 2H, J=5.4 and1.4 Hz), 5.29 (t, OH, $J_{H,OH}$= 5.4 Hz). **^{13}C-NMR** (150.87) MHz, decoupled with ^{1}H**,** coupled with ^{19}F**,** DMSO) δ_C(ppm): 52.9, 55.2, 66.8, 116.1, 118.3, 120.12, 122.36.**^{19}F-NMR** (564.04 MHz, DMSO)δ_F(ppm): – 78.97(s, (CF_3).

In the ^{1}H-NMR spectrum, the single intensepeak at 3.10 ppm corresponds to nine protons (H_a) of three methyl groups bounded to the nitrogen atom [($C\mathbf{H}_3)_3N^+CH_2CH_2OH$] with an integration of around 9.00 which have the same chemical and magnetic equivalence. The triplet at 3.40 ppm indicates protons (H_b) of methylene groups [$(CH_3)_3N^+C\mathbf{H}_2CH_2OH$], while the methylene protons (H_c)[$(CH_3)_3N^+CH_2C\mathbf{H}_2OH$] are centred at 3.83 ppm. Both triplets have an integration of around 2.00. On the other hand, the signal at δ =5.29 ppmwith an integration of around 1.00can be attributed to the proton (H_d) of hydroxyl group in the choline cation [$(CH_3)_3N^+CH_2CH_2O\mathbf{H}$].The appearance of this signal as a triplet indicates that the –OH group of ([$CHOL^+$]) was coupled with adjacent protons of the CH_2 throught the C-O-H. The agreement of these integration values evidence the structure of [$CHOL^+$][$(CF_3SO_2)_2N^-$] and its high purity.Note thatthe experimental^{13}C-NMR spectrum decoupled with ^{1}H but non decoupled with ^{19}F also further corroborate the structure of ([$CHOL^+$]) cation. Moreover, one finds a quartet (intensity 1,3,3,1) at 116.1, 118.3, 120.1, 122.4 ppm, consistently with the expected signals of the ([NTf_2^-]) anion, δ = 119.21 ppm with $J_{C-F}\simeq$312 Hz [43]. Furthermore, ^{19}F-NMR spectrum presents a singlet at δ= -78.97 ppm, in agreement with the presence of F atoms.This demonstrate the effectiveness of the anionic reaction.

Figure 1. Experimental Hydrogen atom labeling and ^{1}H-NMR spectrum of [$CHOL^{+}$][$(CF_3SO_2)_2N^{-}$].

Figure 2. Experimental ^{13}C-NMR spectrum of [$CHOL^{+}$][$(CF_3SO_2)_2N^{-}$].

Figure 3. Experimental ^{19}F-NMR spectrum of [$CHOL^{+}$][$(CF_3SO_2)_2N^{-}$].

The computed^{1}H,^{13}C and ^{19}F-NMR chemical shifts are reported in Tables 1, 2 and 3, where they are compared with the experimntal values. The predicted values for the F atoms of anion and IL were obtained using CCl_3-F as reference. The optimized structures of cation, anion and IL are reported in **Figure 4**.

Figure 4. Optimized structures of cation, anion and [$CHOL^{+}$][$(CF_3SO_2)_2N^{-}$] ionic liquid in gas phase by using the B3LYP/6-311G** level of theory showing the formation of intra-molecular H bond between anO atom of S=O group and the H atom of OH group.

Experimental and computed values showbetter agreement for the ^{1}Hand ^{19}F nucleui of the IL (0.57 and 21.62 ppm) than of the cation (1.01 and 32.75 ppm) while, on the contrary, for the ^{13}C nucleus a higher RMSD value is observed for IL (7.16 ppm) as compared to value of cation (4.32 ppm). From the good concordances observed for the ^{1}H and ^{13}C nucleus the molecular structure of IL was confirmed despite the lower correlations observed for the ^{19}F nucleus, as also was observed for the same anion in ILs with different cations [21,22].The high RMSD observed for the ^{19}F nucleus could be justified by the predicted C-F⋯H interactions, as we will see in the next section. In general, the observed variations could be ascribed to different solvent used and to other types of interactions in solution not considered in the calculations.

3.2. Optimizations in gas phase and aqueous solution

Figure 4 shows the optimized structure of [$CHOL^{+}$][$(CF_3SO_2)_2N^{-}$] IL in which one can note an intra-molecular H bond between the O atom of a SO_2 group of [$(CF_3SO_2)_2N^{-}$] and hydrogen atom of OH group of [$CHOL^{+}$]. **Table 4** shows the calculated total energies, volume (V) and dipole moment (μ) of the IL, anion and cation in different media. The anion presents higher μ and V in the two media than the cation and both species increase these values in the IL. Higher μ and V values are observed for the IL in solution (24.19 D and 317.6 Å^3), as compared tothe gas phase (14.22 D and 311.5Å^3). In solution, the cation and IL show a volume expansion, as a consequence of the increase in their μ values, while the anion decreases its V in water. **Figure S1** shows the different magnitudes, directions andorientations of the μvectorsof the three species. The vectors of cation and anion are shown

in gas phase while for the IL they are reported in both media. In the IL the vector is oriented from the N of anion to the N of cation changing the direction and orientation in solution. Moreover, one can note that the values of total energies corrected by the Zero-point vibrational energy (ZPVE) are less negative than the non corrected ones, as observed in other ILs [21,22].The difference between the uncorrected energy of the IL (-2156.5257 Hartrees) and the sum of the energies of the isolated cation and anions (-328.7894 and - 1827.6092= -2156.3986 Hartrees)is the interaction energy between the ions.

Table 5 shows some predicted distances in the IL: the closest distances between anion and cation involveS2-O3···H18 (1.832Å) and S9-O10···H25 (2.160 Å)in the gas phase while in solution the closest distance is that of the former groups (1.948 Å. In Table 5 it is possible to observe short C-F···H distances, which can justify the high ^{19}F chemical shifts predicted for IL.

In **Table 6**the geometrical parameters for the IL calculated in the two media are compared with the corresponding experimental ones reported in Ref [19] in the solid state. A better agreement is found for distances (0.055-0029 Å) than for angles (1.8-1.3 °). The values calculated in solution display in general a lower agreement with the experiments. Regarding the values, it is observed that the predicted bond O3-H18 lengths in both media (1.832, 1.948 Å) are different from the experimental one (1.703 Å), possibly because of the formation of hydrogen bonds in the real system. Also, as a consequence of cation-anion interactions the bond S2-O3-H18 angles change from 137.4 ° in gas phase to 130.0 ° in solution while the experimental value is slight lower (127.8 °). Thus, from Fig. 4 we observed the formation of S2-O3···H18 interaction and, for this reason, the related parameter (N1-S2-O3) changes notably in both media. On the other hand, few change is observed in the S2=O3 bond length (1.473 Å) in gas phase; however, a lower value (1.469 Å) than the experimental one (1.475 Å) is observed in solution. Obviously, the heavier S and O atoms are more difficult to modify than lighter H ones. The parameters related to CF_3 groups of anion and the quaternary N16 atoms of cation have extremely small changes in both media. However, in solution, the geometrical parameters of N1 atoms change probably because the lone pairs could be hydrated.

3.3. Atomic charges, molecular electrostatic potentials and bond orders

The Mulliken, Merk-Kollman (MK) and atomic natural population analysis (NPA) charges for all atoms of IL are compared in **Table S1**. The graphic comparison of the charges of N, C, O and F atoms are displayed in **Figure S3**. The variations of MK and NPA charges on those atoms follow practically the same behaviours in both media. Small values of Mulliken

changes are calculated in a vacuum, while, on the contrary, some changes in these values occur in solution. The Mulliken charges on on S2 increases in gas phase while it decreases on S9.The MK charge on quaternary N16 is positive in both media , as expected for the cation, while NPA and Mulliken charge is negative. The values of NPA and MK charges of O, C and F show little change with the medium. In this study, the three types of charges in the two media show on N1 negative values, which are expected since that atom belongs to the anion.

To analyse the reaction sites in the IL and, also the strength of different bonds, the bond orders (BO) expressed as Wiberg indexes and the molecular electrostatic potentials (MEP)have been studied in both media. **Table S2** shows the two parameters for the $[CHOL^+][(CF_3SO_2)_2N^-]$IL in the two media. The MEP values change as expected considering the electronegativity of the atoms in the order F> O > S > N > C> H. The O atoms of the anion display the higher variations (0.055-0.019 a.u.) passing from vacuum to solution, while for the S (0.023 a.u.) and C (0.017-0.015 a.u.) atoms, lower values are predicted. Moreover, the lowest MEP values are calculated for the most labile atoms in both media (H18); hence, it is clear that this atom forms an H bond with the O3 atom of SO_2 group belonging to anion. Figure S3 reports the MEP surfaces of IL in the two media and one can visualize (i) the various electrophilic and nucleophilic sites of reaction and, (ii) the notable reduction of the energy in solution. The value decreases from 0.074 a.u.in vacuum to 0.011 a.u. in solution. From figure S3 it is observed that the regions corresponding to cationpresents blue colours and are electrophilic, which is expected because it is positively charged, while the red colours corresponding to anion are located on the O atoms and are the nucleophilic sites.

The bond orders (BO) by atom, expressed as Wiberg indexes,for the IL in the two media are displayed in Table S2:the values of all the atoms change in solution, with the exception of S2 and H36 atoms that have similar values independently of the medium. The slight differences observed in these values could be related to the formation of hydrogen bonds in solution..

3.4. NBO and AIM calculations

The investigation of stability of $[CHOL^+][(CF_3SO_2)_2N^-]$in the two media is highly important, especially considering the hydrogen bond network which develops in the IL. Here, the stabilities of IL have been studied by using:(i) the acceptor-donor interactions energies (E2) calculated with the Second Order Perturbation Theory Analysis of Fock Matrix in NBO Basis [32] and(ii) by using the Bader's theory of atoms in molecules with the AIM 2000 program [33,34]. **Table S3**reports the E2 values [32]. Two different types of interactions are expected for the IL , as previously observed in other ILs [21,22]. The first one is the$n \rightarrow \sigma^*$ interaction

between the lone pairs of O, N and F atoms of [$(CF_3SO_2)_2N^-$] to various anti bonding S-O, S-N, S-C, and C-F orbitals. The second type of interaction is the $\sigma^* \rightarrow \sigma^*$ one that involves the anti bonding S-O orbitals (see Table S3). The total energy is 1762.0 kJ/mol in vacuum and 1950.1 kJ/mol in solution. The similarity of these values point towards a similar stability of the IL in the two media, even though it seems slightly more stable in solution.

The AIM 2000 program [33,34] was used to investigate the topological properties of the IL in the various critical points. Table S4 reports the main interactions while Table S5 summarize the main values of the topological properties found both in gas and in solution phases. Figure S4 reports the location of the critical points. The new interactionsS9-O10⋯H25 and C19-H22⋯N1 in gas phase and, C12-F13⋯H25 in solution are shown in **Table S6**. Both NBO and AIM investigations suggest a good stability of [$CHOL^+$][$(CF_3SO_2)_2N^-$], independently of the medium.

3.5. Frontier Orbitals calculations

The frontier orbitals and their differences are calculated to obtain the gap values and the reactivity of the IL. The global softness (S), hardness (η), and electrophilicity (ω) were calculated (see **Table S7**).For comparison, the same parameters were computed for the isolated ions. The gap of the cation largely exceeds that of the anion, while in the ionic couple one has an intermediate value, which is higher in solution(7.4640 eV) than in the gas phase (6.5360 eV); therefore, the IL is more reactive in vacuum and more stable in solution. Comparing the gap values of [$CHOL^+$] [$(CF_3SO_2)_2N^-$] IL with those reported for [C_8DABCO^+][$(CF_3SO_2)_2N^-$] (6.7756 eV in gas phase and 5.7389 eV in solution) it is clear that this latter IL is more reactive in solution while the former is more reactive in gas phase [22]. Here, the [C_8DABCO^+] cation increases the reactivity of [C_8DABCO^+][$(CF_3SO_2)_2N^-$] in solution while [$CHOL^+$] increasesthereactivityof [$CHOL^+$][$(CF_3SO_2)_2N^-$] in gasphase. The frontier orbitals of [$CHOL^+$][$(CF_3SO_2)_2N^-$] in the two media are reported in **Figure S5**; one can observe that the anion orbitals participate in the HOMO in gas phase but not in solution while the contrary is observed in the LUMO. The cation is involved in the HOMO in solution. Evidently, the different participations of HOMO and LUMO in the media justifies the higher reactivity of IL in vacuum and its higher stability (< reactivity) in solution. Consistently, the global electrophilicity index ω(3.1743 eV) in higher in the gas phase.

3.6. Vibrational study

We used calculation to optimize the structure of $[CHOL^+][(CF_3SO_2)_2N^-]$ IL with C_1 symmetry, with the SO_2groups in opposite positions and with the CF_3 groups in *Trans* positions, as shown in Figure 4.In this IL, the presence of 36 atoms generates a total of 102 normal vibration modes, all a of them both Raman and infrared active. The experimental infrared and Raman spectra in the solid phase are compared respectively in **Figures 5** and **6** with the spectra calculated for the ionic couple, the cation and anion in vacuum. Calculated and experimental spectra show a good correlation, especially the Raman one. Clearly, Figure 5 displays that the observed IR bands of IL in the region of higher wavenumbers are due to cation while the bands between2000 and 10 cm^{-1} are due to cation and anion species. The theoretical infrared spectrum of IL, cation and anion are reported in **Figure S6**. The scaled quantum mechanical force field (SQMFF) method allowed to obtain the harmonic force fields of the ionic couple in the two media, by means of the MOLVIB suite [38-40]. For the IL and the cation the normal internal coordinates and transferable scaling factors were used while for the anion the normal internal coordinates of anion were obtained from the literature [22].A good agreement between the calculated and measured bands is observable in Table7, where also the assignment of the vibrations is reportedOne can note in Table 7, that due to the formation of hydrogen bonds between the two ions, the cation vibrational bands are displaced toward lower frequencies in the IL. The main assignments of the vibrational bands are reported in the following.

Figure 5. Experimental FT-IR spectrum of IL in the solid phase compared with the corresponding predicted for IL and its cation and anion in the gas phase by using the hybrid B3LYP/6-311++G** level of theory.

3.6.1. Vibrational band Assignment

3.6.1.1. 4000-2000 cm^{-1} region. The OH stretching and the symmetric and antisymmetric stretching of CH_2 and CH_3 groups of the cations are expected [21,22] in this region. Calculations predict that the bands of the IL can be found at lower wavenumbers with respect to those of the cation, due to the interaction between the ions, as it was observed in other IL [22]. Moreover, the SQM calculations predict different assignments for the cation and the IL, due to the interaction between the ions, as previously investigated by NBO and AIM calculations. The assignment of the infrared and Raman bands observed in this region are displayed in Table 7. It can be noted that this IL does not possess intense Raman bands;

therefore, hence, the symmetric $CH_2$and CH_3stretching modes are assigned in the expected positions according to the SQM calculations.

3.6.1.2. 2000-1000 cm^{-1}spectral range. In this spectral range, the vibration modes of cation and IL, such as CH_3 and CH_2 deformation, OH deformation, CH_2 wagging, CH_3 and CH_2 rocking modes are expected in addition to SO_2 and CF_3 stretching modes of anion [21,22]. According to SQM calculations, the observed bands in the range 1507-1058 cm^{-1} are ascribed to CH_3 and CH_2 deformation, CH_2 wagging, CH_3 and CH_2 rocking modes of the cation.Then, the interaction of cation with the anion leads to the shifting toward lower wavenumber of SO_2 stretching modes involved in the H bond interaction. Hence, in the anion the symmetric stretching mode $\nu_s SO_2$ (S2) is expected at 1056 cm^{-1} while in the IL that mode is calculated at 1029 cm^{-1}. Also, the antisymmetric mode in the anion is predicted at 1236 cm^{-1} while in the IL at 1234 cm^{-1}.However, the stretching modes of CF_3 groups remain practically in the same positions because these groups are involved in weak H bond interactions. The OH deformation mode in the cation is expected at 1164 cm^{-1}; on the contrary in the IL this mode is predicted in different positions and coupled with other modes due to participation of this group to strong S2-O3···H18interactions. The very strong infrared active bands centered at 1197 and 1149 cm^{-1} are ascribed to deformation and torsion of OH group, as well as to the stretching modes of CF_3groups (see Table 7).Finally, the very strong IR band at 1071 cm^{-1} is assigned to C-O and C-C stretching modes of cation and IL.

3.6.1.3. 1000-10 cm^{-1} region. In this region, one can observe the CH_2 and CH_3 twisting and C-C, C-N and S-N stretching, as well as and CCC, CCN, skeletal modes of cation together with vibration modes of anion [21,22]. The CH_2 twisting modes are poorly influenced by the anion and are expected in the cation between 1053 and 843 cm^{-1} while in the IL between 960 and 847 cm^{-1}. Here, it is observed that the SO_2wagging, rocking and twisting modes related to the S2-O3···H18 interaction are predicted in the IL at a higher wavenumber than in the to cation due to H bond. The vibration modes of CF_3 groups are poorly influenced by the cation and, thus, these modes in the IL are observed in the same regions observed for the anion.

Figure 6. Experimental FT-Raman spectrum of IL in the solid phase compared with the corresponding predicted for IL and its cation and anion in the gas phase by using the hybrid B3LYP/6-311++G** level of theory.

3.7. Scaled force constants

Scaled force constants for the $[CHOL^+][(CF_3SO_2)_2N^-]$ ionic liquid and its cation and anion in vacuum and solution were calculated at the B3LYP/6-311++G** level of theory/basis set

because these parameters show how the interactions influence the geometrical parameters and vibration modes. These factors have been obtained from the corresponding harmonic force fields previously reported [38-40].

In **Table 8**wereportthe main scaled internal force constants for the ionic liquid and the cation in the two media while for the [$(CF_3SO_2)_2N^-$] anion the values in vacuum have been taken from previous literature at the same level of theory [22]. Comparing the $f(\nu_{OH})$ force constants of IL and cation, it is observed the decreasing of the values in the IL in the two media due to the formation of S2-O3···H18interaction where that group is involved. Note that all force constants of cation change in the IL as a consequence of interactions, with the exception of $f(\delta_{CH3})$ and $f(\delta_{CH2})$ force constants that show the same values. Hence, the effect of anion on the cation is clearly observed in these parameters. While the values of IL and anion are compared between them, it is observed that the force constants related to SO_2 groups demonstrate higher changes than to those corresponding to CF_3 groups. The observed changes here are attributed to the different interactions predicted by NBO and AIM calculations (see Tables 5, S3 and S4 and Figure S4).

4. Thermal analysis

The thermogravimetric analysis (TGA)of ILs is a powerful means which provides access to information linked to thermal behaviour, namely the degradation temperature[45].On the other hand, low temperature analysis by Differential Scanning Calorimetry (DSC) also makes it possible to determine phase transitions :Freezing, melting, glass transition, cold crystallisation and solid-solid transition temperatures. The curves measured for the mass variation and the heat flux as a function of temperature are presented in Figures 7 and 8.During the rise in temperature, a glass transition around -75°C and three endothermic peaks at 3, 27and 31°Cis observed. The first peak is ascribed to a solid-solid transition of ([$CHOL^+$][$(CF_3SO_2)_2N^-$]), the other two peaks at 27 and 31°C were associated to the melting process. This result agrees with previous study of Villanueva et al. [46].

Figure 7: DSC curve of [$CHOL^+$][$(CF_3SO_2)_2N^-$].

The TGA curve reported in Figure 8 suggests that ([$CHOL^+$][$(CF_3SO_2)_2N^-$]) decomposes in one step, the T_d value of ([$CHOL^+$][$(CF_3SO_2)_2N^-$]) was higher than 400 °C with weight loss was observed starting from T_{id}= 360 °C and was completed at T_{fd}=475°C. The introduction of a bis(trifluoromethanesulfonyl)imide anion resulted in higher T_d values for ([$CHOL^+$][$(CF_3SO_2)_2N^-$]). This result indicates that the thermal stability of the IL is strictly

connected to that of the anion. In addition, it can be noted that the investigated IL exhibited better thermal stability than the halide analogues, containing the Cl or Br anion, thanks to the strong ionic linkage between the cation ([$CHOL^+$]) and the anion ([$(CF_3SO_2)_2N^-$])[47].

Figure 8: TGA curve of [$CHOL^+$][$(CF_3SO_2)_2N^-$].

5. Conclusions

In summary, the synthesis and experimental characterisation of [$CHOL^+$][$(CF_3SO_2)_2N^-$] ionic liquid NMR, infrared and Raman spectroscopy was reported. Structural, topological, electronic and reactivity of IL in vacuum and aqueous solution have been predicted by using B3LYP/6-311++G** calculations. Studies on atomic MK, NPA and Mulliken charges and MEP, NBO and AIM, frontier orbitals have evidenced that the strong S-O···H interaction and other weak H bonds interactionsplay a very important role in determining the properties of this new IL. The MEP surfaces evidenced that the main reactive sites are located on positively charged N^+ of the cation and on the SO_2 groups of the anions. Good agreement is observed between the predicted IR, ^{1}H-NMR and ^{13}C-NMR,and Raman spectra and the experimental ones. A complete assignment of all vibration modes for the IL and its cation is suggested, together with the scaled force constants. In addition, the IL showed its melting temperature near at 30°C while a glass transition and a cold crystallization have been revealed at 3 and -26 °C.

Acknowledgements. This work was supported with grants from CIUNT Project Nº D714 (Consejo de Investigaciones, Universidad Nacional de Tucumán), and with grants from financial support by The Ministry of Higher Education and Scientific Research (MESRS) of Algeria in PRFU project code: B00L01UN200120180002.The authors thank Prof. Tom Sundius for permission to use the MOLVIB program, Also, Prof Haddad boumediene would like to thank (BAKROU Habibo) for their fruitful support.

Supporting Information Available: Tables S1-S4 and **Figures S1-S11**.

Conflicts of interest

All authors declare that there are no conflicts of interest.

References

[1] J.Yu, X.Liu,S. Xu,P. Shao, J. Li, Z. Chen, C. M. Renard, Advances in green solvents for production of polysaccharide-based packaging films: Insights of ionicliquids and deepeutecticsolvents, CRFSFS. 22(2) (2023) 1030-1057,https://doi.org/10.1111/1541-4337.13099.

[2] N. V. P.Veríssimo,C. U.Mussagy, H. B. S. Bento, J. F. B. Pereira, V. de Carvalho Santos-Ebinuma,Ionicliquids and deepeutecticsolvents for the stabilizationof biopharmaceuticals: A review,Biotechnol. Adv. (2024) 108316, https://doi.org/10.1016/j.biotechadv.2024.108316.

[3] L. Y. Zhang, S. H. Liu, Y. Wang, Exploring the influence of the type of anion in imidazoliumionicliquids on its thermal stability, J. Therm. Anal. Calorim.148(11)(2023) 4985-4995,https://doi.org/10.1007/s10973-023-12037-z.

[4] B. Haddad,A.Kachroudi,G.Turky,E. H.Belarbi,A.Lamouri, D. Villemin, A.Sylvestre, The interplaybetweenmolecular structure and dielectricpropertiesinionicliquids: A comparative study, J. Mol. Liq. 324 (2021) 114674, https://doi.org/10.1016/j.molliq.2020.114674.

[5] B. Haddad,S. A.Brandan,M. A.Assenine,A.Paolone, D. Villemin, S. Bresson, Bidentate cation-anion coordination in the ionic liquid 1-ethyl-3-methylimidazolium hexafluorophosphate supported by vibrational spectra and NBO, AIM and SQMFF calculations, J. Mol. Struct. 1212 (2020) 128104, https://doi.org/10.1016/j.molstruc.2020.128104.

[6] A. A. T.Hijo, E. K. Silva,M.Cristianini,A. J.Meirelles, High-intensityultrasoundassisted-emulsificationusingionicliquids as novelnaturally-derivedemulsifiers for foodindustry applications, Innov. Food Sci. Emerg. Technol.84 (2023) 103301,https://doi.org/10.1016/j.ifset.2023.103301.

[7] H. W. Khan,A. A.Elgharbawy,A.Bustam,M.Moniruzzaman,
(2021). Design and selection of ionicliquids via COSMO for pharmaceuticals and medicine. In Application of IonicLiquids in Drug Delivery (pp. 137-164). Singapore: Springer Singapore.
H.W. Khan, A.A. Elgharbawy, M.A. Bustam, M. Moniruzzaman, Design andSelection of IonicLiquids Via COSMO for Pharmaceuticals and Medicine, in:Application of IonicLiquids in Drug Delivery,Springer, Singapore, 2021, pp. 137–164, https://doi.org/10.1007/978-981-16-4365.

[8] A. K.Parameswaran,J.Azadmanjiri,N.Palaniyandy,B. Pal,S.Palaniswami,L. Dekanovsky,Z.Sofer, Recentprogress of nanotechnology in the researchframework of all-solid-state batteries,Nano Energy. 105(2023)107994,https://doi.org/10.1016/j.nanoen.2022.107994.

[9] M. Mirzaei-Saatlo,E.Asghari,H.Shekaari,B. G.Pollet,R.Vinodh, Performance of ethanolamine-basedionicliquids as novel green electrolytes for the electrochemicalenergystorage applications, Electrochim. Acta. 474 (2024) 143499,https://doi.org/10.1016/j.electacta.2023.143499.

[10] K.Morawska,C.Wardak, Application of ionicliquids in ion-selectiveelectrodes andreferenceelectrodes: A review,ChemPhysChem. (2024)e202300818, https://doi.org/10.1002/cphc.202300818.

[11] S. L. Piper,M.Kar, D. R. MacFarlane,K.Matuszek, J. M. Pringle, Ionic liquids for renewable thermal energy storage–a perspective, *Green Chem.*24(1)(2022) 102-117, 10.1039/D1GC03420K.

[12] H. Tian,P.Berton, R. D.Rogers, Choline-based aqueous biphasic systems: Overview of applications,*Fluid Phase Equilib.*502 (2019) 112258, https://doi.org/10.1016/j.fluid.2019.112258.

[13]Y.Liu,X. Yao, H. Yao,Q. Zhou,J.Xin,X. Lu,S.& Zhang, Degradationofpoly (ethyleneterephthalate) catalyzedby metal-free choline-basedionicliquids, *Green Chem.*
22(10)(2020)3122-3131.https://doi.org/10.1039/D0GC00327A .

[14]F.Rabhi,T.Di Pietro,F.Mutelet, H.&Sifaoui, ExtractionoforganiccompoundsfromAqueousSolutionUsingCholine bis(trifluoromethylsulfonyl)imide,*J. Mol. Liq.*360 (2022) 119432.https://doi.org/10.1016/j.molliq.2022.119432 .

[15]U.Domańska,P. Papis,J.&Szydłowski, Thermodynamics and activitycoefficients at infinitedilutionfororganicsolutes, water and diols in theionicliquidcholine bis (trifluoromethylsulfonyl)imide, *J. Chem. Thermodyn.*77(2014)63-70.https://doi.org/10.1016/j.jct.2014.04.024.

[16]L.Cesari,L.Canabady-Rochelle, F. &Mutelet, Extractionofphenoliccompoundsfromaqueoussolutionusingcholine bis(trifluoromethylsulfonyl)imide,*Fluid Ph. Equilibria.*446 (2017) 28-35.https://doi.org/10.1016/j.fluid.2017.04.022 .

[17] Í. F. de Souza,V. H.Paschoal, K. Bernardino, T. A. Lima,L. L.Daemen, M. C. & Ribeiro, Vibrationalspectroscopy and molecular dynamicssimulationofcholineoxyanionssalts, *J. Mol. Liq.*340(2021) 117100.https://doi.org/10.1016/j.molliq.2021.117100.

[18]A. Knorr,K.Fumino,A. M.Bonsa, R. & Ludwig, Spectroscopicevidenceof ‘jumping and peckingofcholinium and H-bond enhancedcation–cationinteraction in ionicliquids, *PCCP.*17(46)(2015) 30978-30982. 10.1039/C5CP03412D.

[19]P.Nockemann,K.Binnemans,B.Thijs,T. N.Parac-Vogt,K.Merz,A. V.Mudring,C.&Glorieux, Temperature-drivenmixing-demixingbehaviorofbinary mixtures oftheionicliquidcholine bis(trifluoromethylsulfonyl)imide and wáter, *J. Phys. Chem. B.*113(5)(2009) 1429-1437.https://doi.org/10.1021/jp808993t.

[20]Y. Zhuravlev,K.Gordienko,D. Dyagilev,S.Luzgarev,S.Ivanova,A.&Prosekov, Structural, electronic, and vibrationalpropertiesofcholinehalides, *Mater. Chem. Phys.*246(2020) 122787. https://doi.org/10.1016/j.matchemphys.2020.122787.
[21]B. Haddad,S. A.Brandán,B.Fetouhi,A.Paolone,M.Boumediene,D.,Villemin, S.&Bresson, Synthesis, NMR, IR, Ramanspectra and DFT calculations of 1-octyl-1, 4-diazabicyclo [2.2. 2] octan-1-ium bis(trifluoromethylsulfonyl)imide, *J. Mol. Struct.*1288 (2023) 135792.https://doi.org/10.1016/j.molstruc.2023.135792.
[22]M. A.Assenine,B.Haddad,A.Paolone,S. A.Brandán,M.Goussem,D.,Villemin, S.&Bresson, Synthesis, termal properties, vibrationalspectra and computationalstudiesofTrioctylmethylammonium-bis(trifluoromethylsulfonyl)imideionicliquid, *J. Mol. Struct.*1232 (2021) 130085.https://doi.org/10.1016/j.molstruc.2021.130085.
[23]M. Boumediene,B.Haddad,A.Paolone,M.Drai,D.Villemin,M.Rahmouni, O.& Abbas, Synthesis, termal stability, vibrationalspectra and conformationalstudiesof novel dicationic meta-xylyllinked bis-1-methylimidazoliumionicliquids, *J. Mol. Struct.*1186 (2019) 68-79.https://doi.org/10.1016/j.molstruc.2019.03.019.
[24] A.D. Becke, Density-functional exchange-energy approximation with correctasymptoticbehavior, *Phys. Rev. A.*38 (6) (1988) 3098–3100. https://doi.org/10.1103/physreva.38.3098.
[25] C. Lee, W. Yang, R.G. Parr, Development of the Colle-Salvetti correlation-energyformula into a functional of the electron density, *Phys. Rev. B.*37 (1988) 785–789. https://doi.org/10.1103/physrevb.37.785.
[26] GaussView, version 6.1.1, R.D. Dennington, T.A. Keith, J.M. Millam, Semichem Inc., Shawnee Mission, KS, 2019.
[27] Gaussian 16, Revision C.01, M.J. Frisch, G. W. Trucks, H.B. Schlegel, G.E. Scuseria, et al, Inc., Wallingford CT, 2019.
[28] S. Miertus, E. Scrocco, J. Tomasi, Electrostatic interaction of a solute with acontinuum, *Chem. Phys.* 55 (1981) 117–129. https://doi.org/10.1016/0301-0104(81)85090-2.
[29] J. Tomasi, J. Persico, Molecular interactions in solution: an overview ofmethods based on continous distributions of the solvent, *Chem. Rev.* 94 (1994)2027–2094. https://doi.org/10.1021/cr00031a013.
[30] A.V. Marenich, C.J. Cramer, D.G. Truhlar, Universal solvation model based onsolute electron density and a continuum model of the solvent defined by the bulkdielectric constant and atomic surface tensions, *J. Phys. Chem. B.*113 (18) (2009)6378–6396. https://doi.org/10.1021/jp810292n.
[31] P. Ugliengo, MOLDRAW Program, University of Torino, DipartimentoChimicaIFM,Torino, Italy, 1998.
[32] E.D. Glendening, J.K. Badenhoop, A.D. Reed, J.E. Carpenter, F. Weinhold, NBO 3.1;Theoretical Chemistry Institute, University of Wisconsin, Madison, WI, 1996.
[33] R.F.W. Bader, Atoms in Molecules, A Quantum Theory, Oxford University Press,Oxford, 1990, ISBN 0198558651.
[34] F. Biegler-Köning, J. Schönbohm, D. Bayles, AIM 2000; A program to Analyze and Visualize atoms in molecules, *J. Comput. Chem.* 22 (2001) 545. https://doi.org/10.1002/1096-987X(20010415)22:5<545::AID-JCC1027>3.0.CO;2-Y.
[35] B.H. Besler, K.M. Merz Jr, P.A. Kollman, Atomic charges derived fromsemiempirical methods, *J. Comput. Chem.* 11 (1990) 431–439. https://doi.org/10.1002/jcc.540110404.
[36] R.G. Pearson, Absolute electronegativity and hardness correlated with molecularorbital theory, *Proc. Natl. Acad. Sci. U.S.A.* 83 (1986) 8440–8441. https://doi.org/10.1073/pnas.83.22.8440.
[37] R.G. Parr, L.V. Szentpaly, S. Liu, Electrophilicity index, *J. Am. Chem. Soc.* 121(1999) 1922–1924. https://doi.org/10.1021/ja983494x.
[38] P. Pulay, G. Fogarasi, G. Pongor, J.E. Boggs, A. Vargha, Combination of theoretical ab initio and experimental information to obtain reliable harmonic force constants. Scaled quantum mechanical (QM) force fields for glyoxal, acrolein, butadiene, formaldehyde, and ethylene. *J. Am. Chem. Soc.* 105 (1983) 7073.https://doi.org/10.1021/ja00362a005.
[39] G. Rauhut, P. Pulay, Transferable Scaling Factors for Density Functional Derived Vibrational Force Fields. *J. Phys. Chem.* 99 (1995) 3093-3100.https://doi.org/10.1021/j100010a019.
[40] T. Sundius, Scaling of ab-initio force fields by MOLVIB. *Vib. Spectrosc.* 29 (1-2) (2002) 89-95. https://doi.org/10.1016/S0924-2031(01)00189-8.
[41] G. Keresztury, S. Holly, G. Besenyei, J. Varga, A.Y. Wang, J.R. Durig. Vibrational spectra of monothiocarbamates-II. IR and Raman spectra, vibrational assignment, conformational analysis and ab initio calculations of S-methyl-N, N-dimethylthiocarbamate,*SAA.*49(13-14) (1993) 2007-2026. https://doi.org/10.1016/S0584-8539(09)91012-1.
[42] R. Ditchfield, Self-consistent perturbation theory of diamagnetism. I. A gauge-invariant LCAO (linear combination of atomic orbitals) method for NMR chemical shifts, *Mol Phys.* 27 (1974) 714–722. https://doi.org/10.1080/00268977400100711.

[43] L. L. Tolstikova, A. V. Bel'skikh, and B. A. Shainyan,Trifluoromethanesulfonate, Trifluromethylsulfonylimide, and Bis(trifluoromethylsulfonyl)imide Salts and IonicLiquids Based on 1,8-Diazabicyclo[5.4.0]undec-7-ene and 1,5-Diazabicyclo[4.3.0]non-5-ene*Russian Journal of OrganicChemistry*, *46*,*(*2010) 383–388.https://doi.org/10.1134/S1070428010030140

[44] B. Haddad, S. A.Brandán, B.Fetouhi,M. Boumediene,A.Paolone,D. Villemin, S. &Bresson, Synthesis, NMR, vibrational spectroscopy, thermal and DFT studies of new DABCO hexafluorophosphate based ionic liquid, *J. Mol. Struct.*1258 (2022) 132682.https://doi.org/10.1016/j.molstruc.2022.132682 .

[45] B. Haddad,D. Villemin,E. H. &Belarbi, Synthesis, Differential Scanning Calorimetry (DSC) and Dielectric Relaxation Spectroscopy (DRS) Studies of N-methyl-N-propylpiperidiniumBis(trifluoromethylsulfonyl)imide, *Environ. Sci.*3(2012)312-319.

[46] M. Villanueva,J. J.Parajó,P. B. Sanchez,J. García, J. & Salgado, Liquid range temperature of ionic liquids as potential working fluids for absorption heat pumps, *J. Chem. Thermodyn.*91(2015) 127-135.https://doi.org/10.1016/j.jct.2015.07.034 .

[47] B. Haddad,M. Boumediene,B.Khalili,K.Ghauri,A.Paolone,S.Taibi, S.&Bresson, Synthesis, vibrational and thermal studies of new 3, 3′-dibutyl-1, 1′-(1, 4-phenylenedimethylene)-bis (1H-imidazolium) ionic liquids: an experimental and quantum computational investigation, *J. Mol. Struct.* (2023) 137325. https://doi.org/10.1016/j.molstruc.2023.137325 .

Figure Captions

Scheme 1. General synthesis of Choline bis(trifluoromethylsulfonyl)imide

Figure 1. Experimental Hydrogen atom labeling and ^{1}H-NMR spectrum of [$CHOL^{+}$][$(CF_3SO_2)_2N^{-}$].

Figure 2. Experimental ^{13}C-NMR spectrum of [$CHOL^{+}$][$(CF_3SO_2)_2N^{-}$].

Figure 3. Experimental ^{19}F-NMR spectrum of [$CHOL^{+}$][$(CF_3SO_2)_2N^{-}$].

Figure 4. Optimized structures of cation anion and IL by using the hybrid B3LYP/6-311++G** level of theory.

Figure 5. Experimental FT-IR spectrum of IL in the solid phase compared with the corresponding predicted for IL and its cation and anion in the gas phase by using the hybrid B3LYP/6-311++G** level of theory.

Figure 6. Experimental FT-Raman spectrum of IL in the solid phase compared with the corresponding predicted for IL and its cation and anion in the gas phase by using the hybrid B3LYP/6-311++G** level of theory.

Figure 7: DSC curve of [$CHOL^{+}$][$(CF_3SO_2)_2N^{-}$].

Figure 8: TGA curve of [$CHOL^{+}$][$(CF_3SO_2)_2N^{-}$].

Figure(s)

Click here to access/download;Figure(s);figure 1 NMR H.tiff

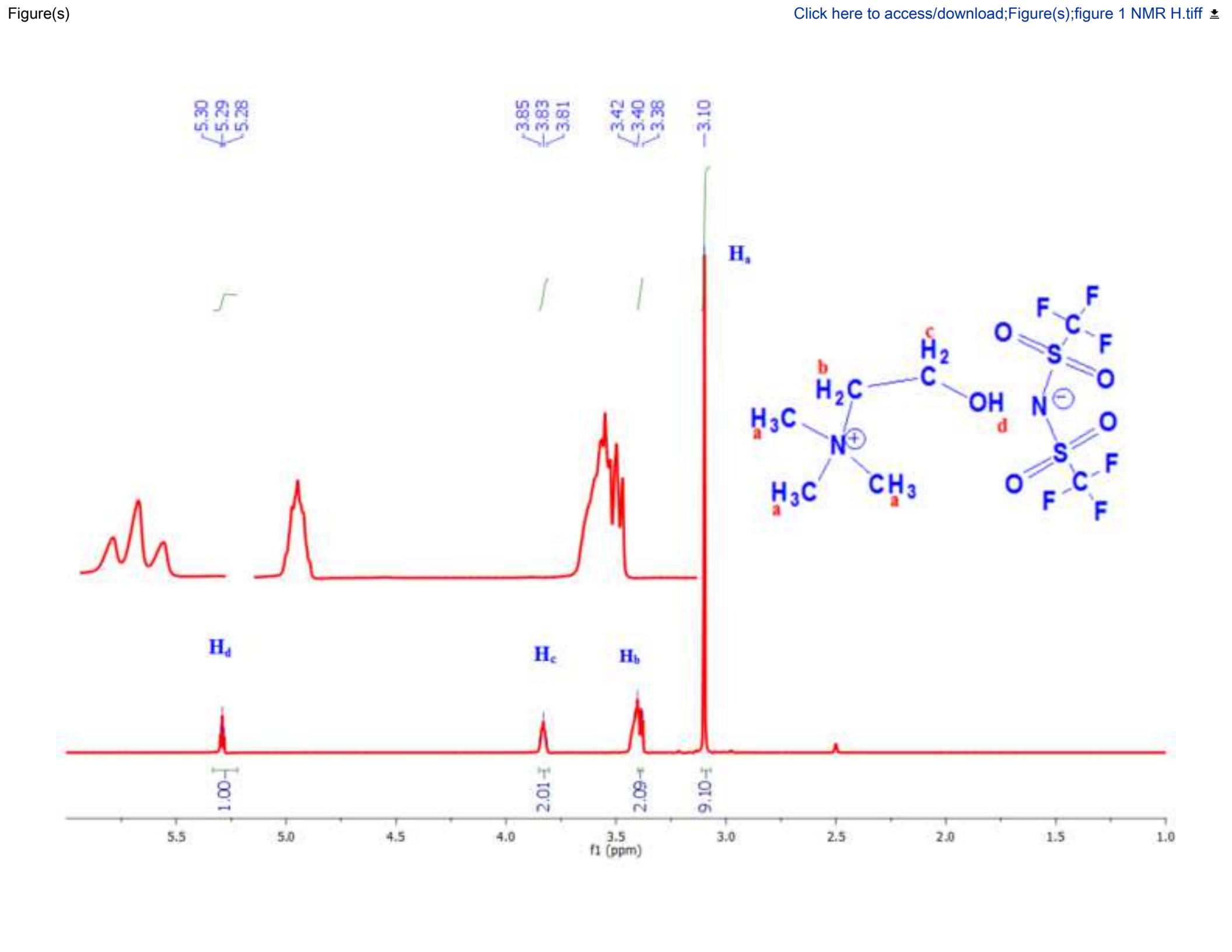

Figure(s)

Click here to access/download;Figure(s);Figure 2 NMR C.tiff

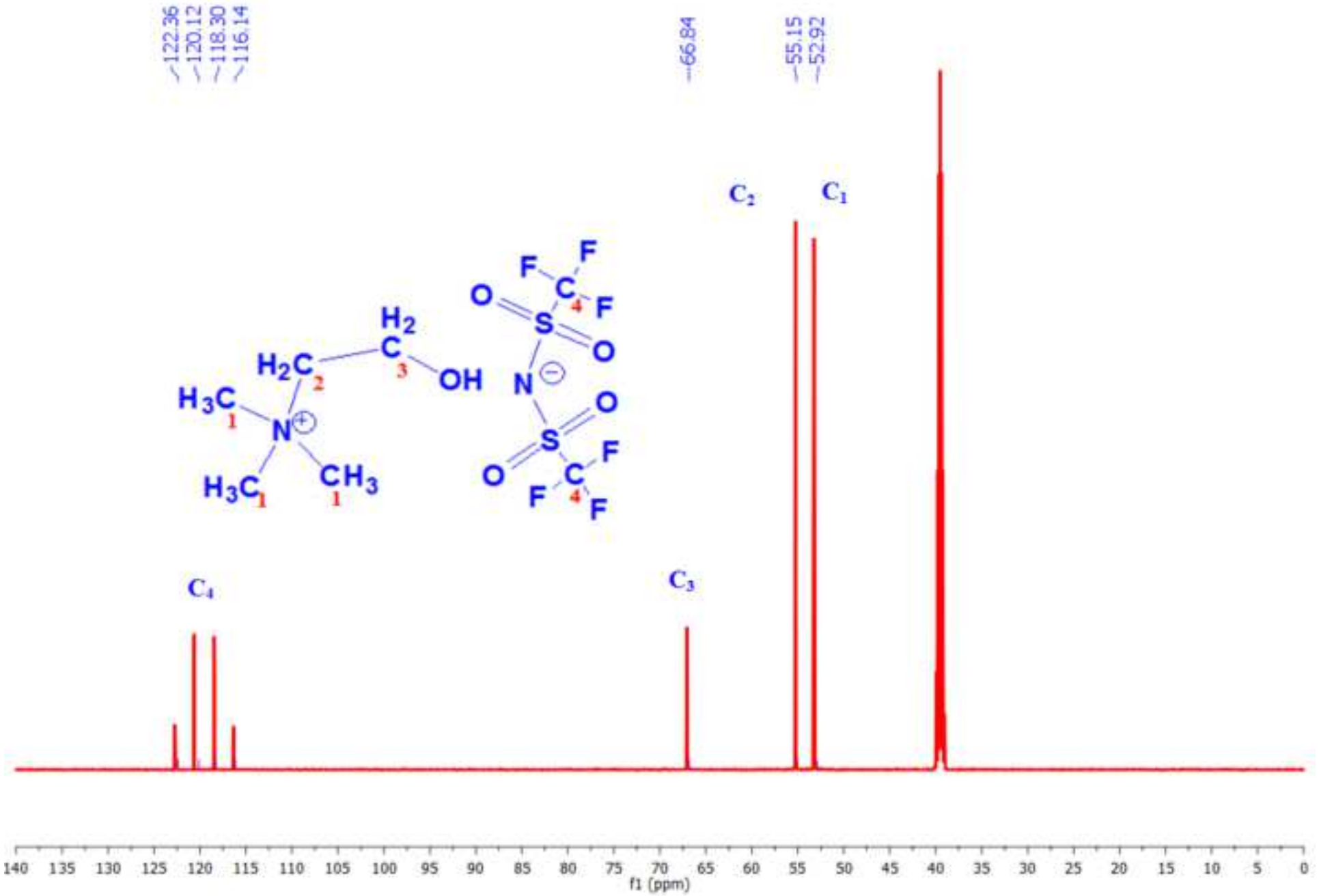

Figure(s)

Click here to access/download;Figure(s);Figure 3 NMR F.tiff

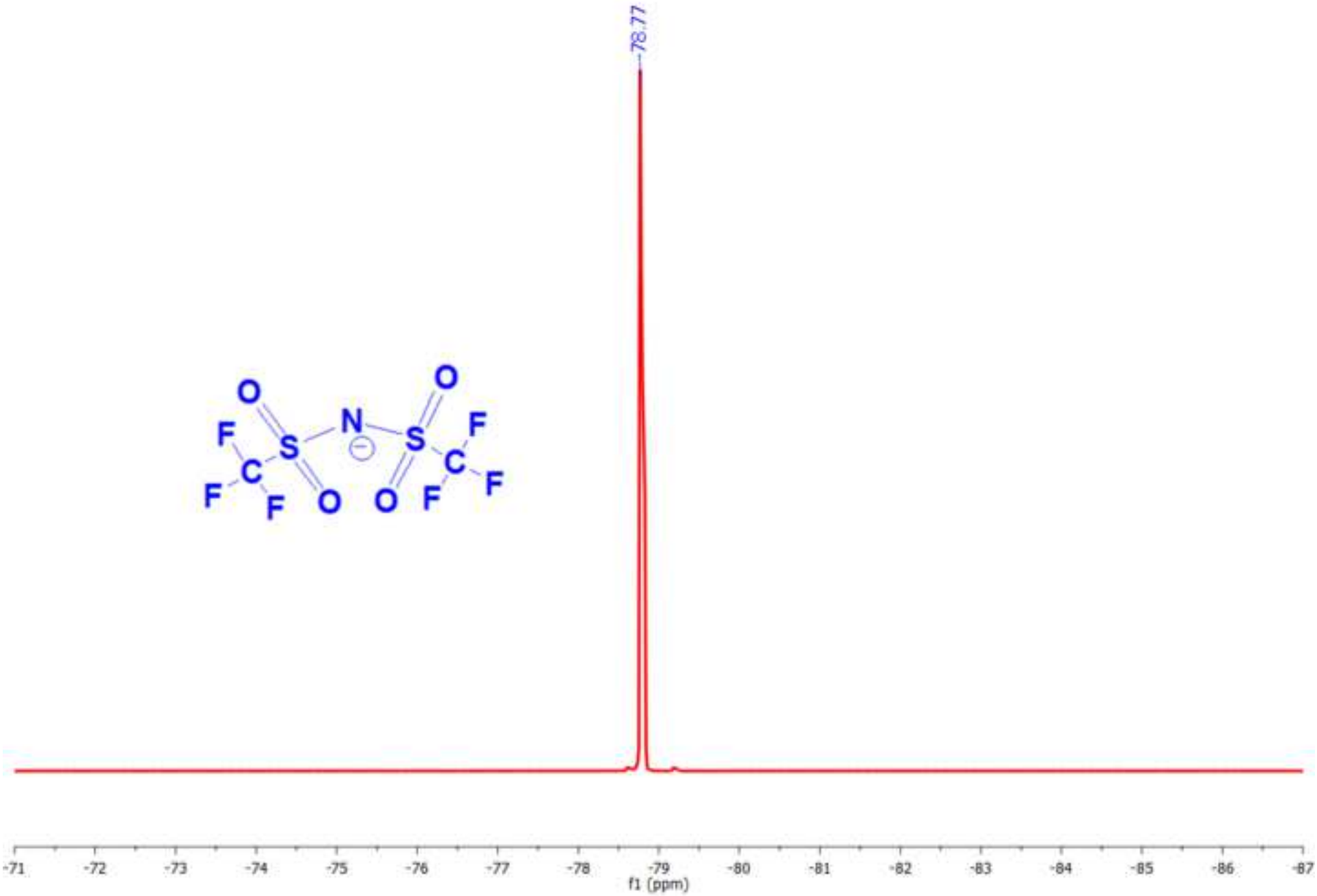

[CHOL$^+$]

[$(CF_3SO_2)_2N^-$]

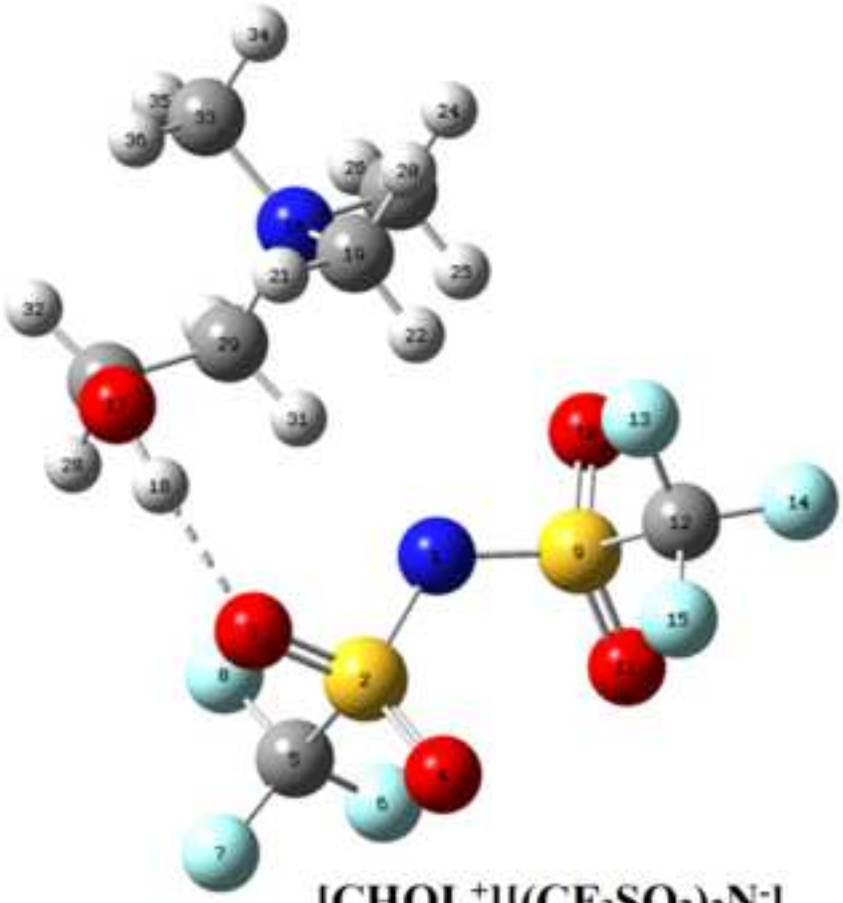

[CHOL$^+$][$(CF_3SO_2)_2N^-$]

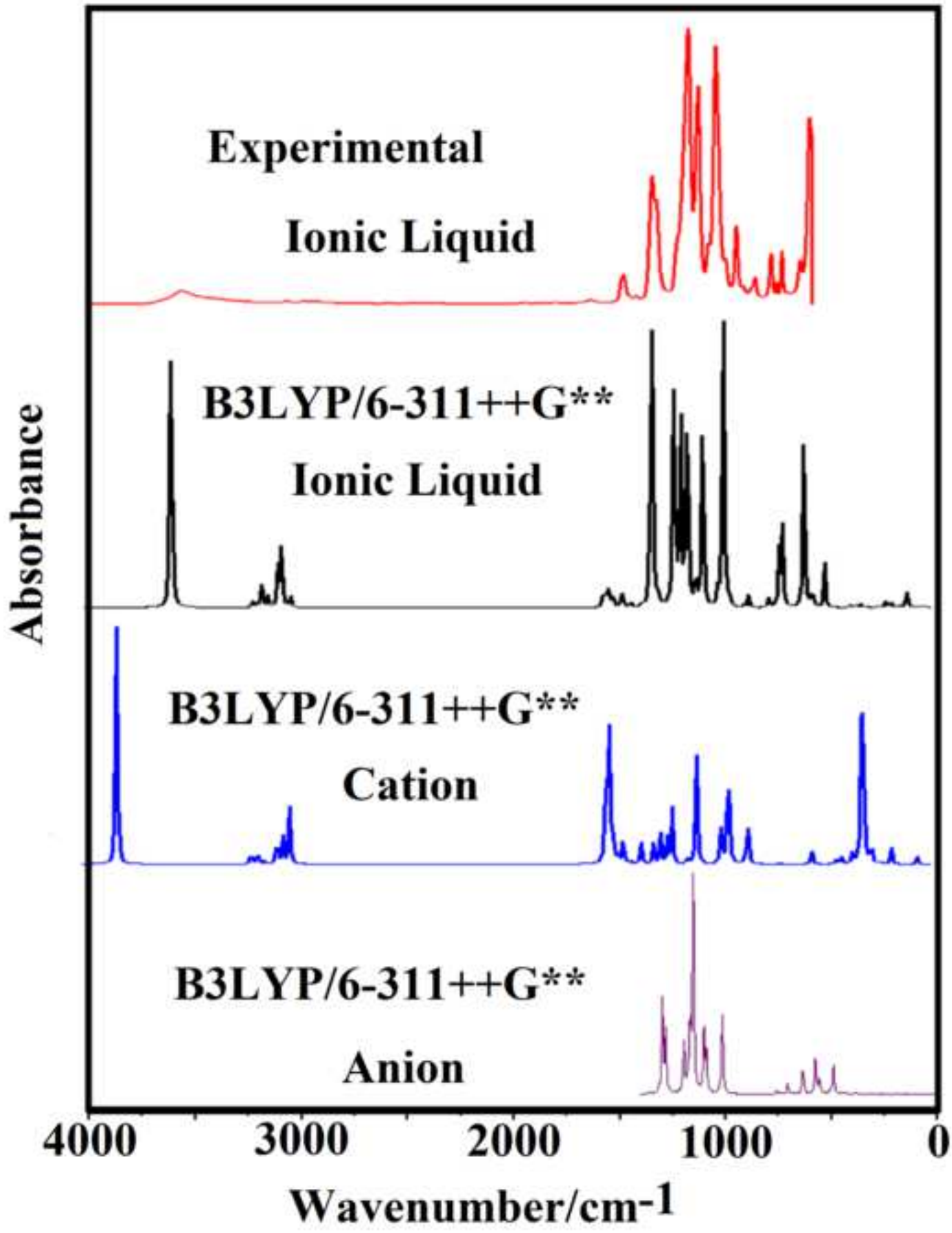

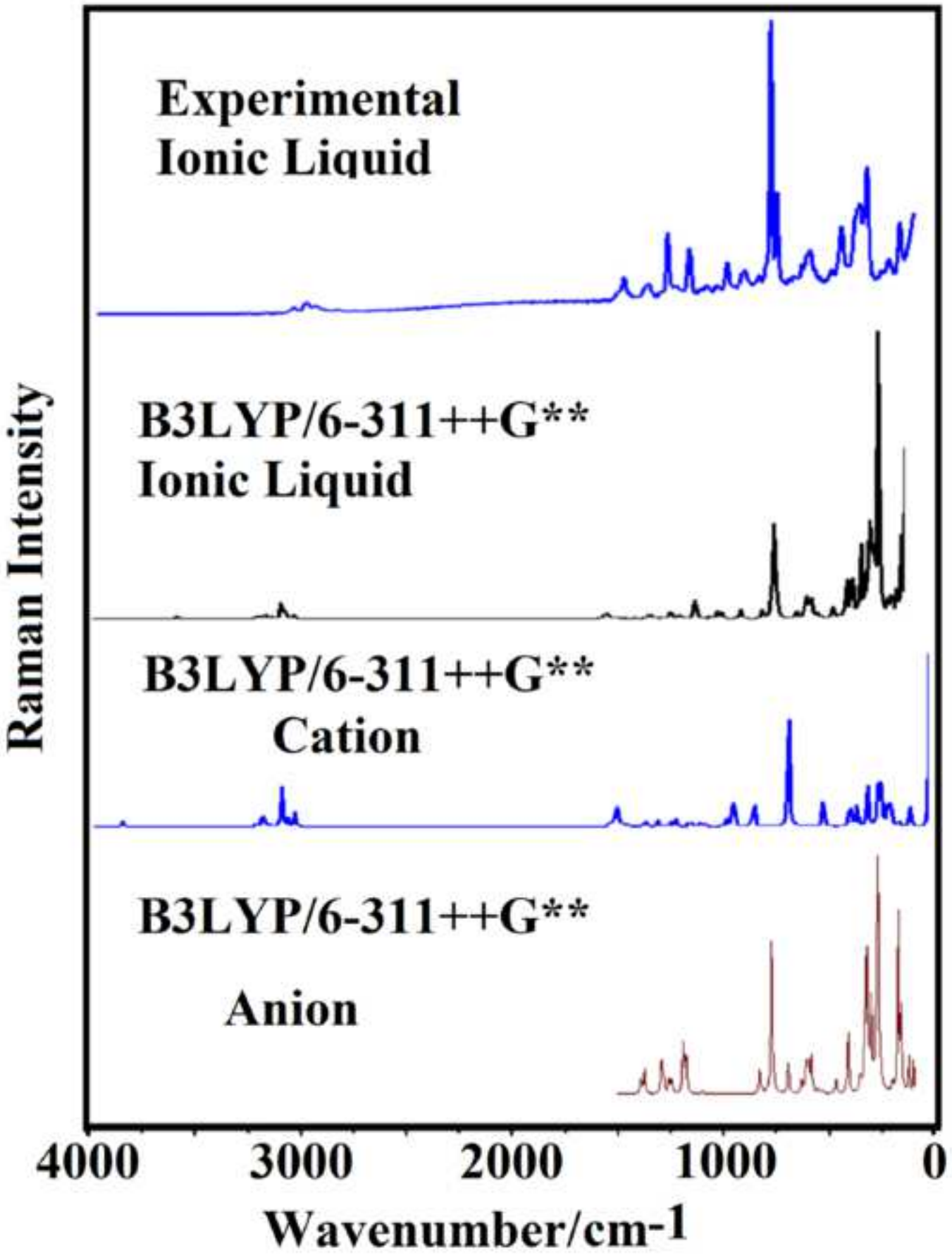

Figure(s)

Click here to access/download;Figure(s);Figure 7 DSC.gif

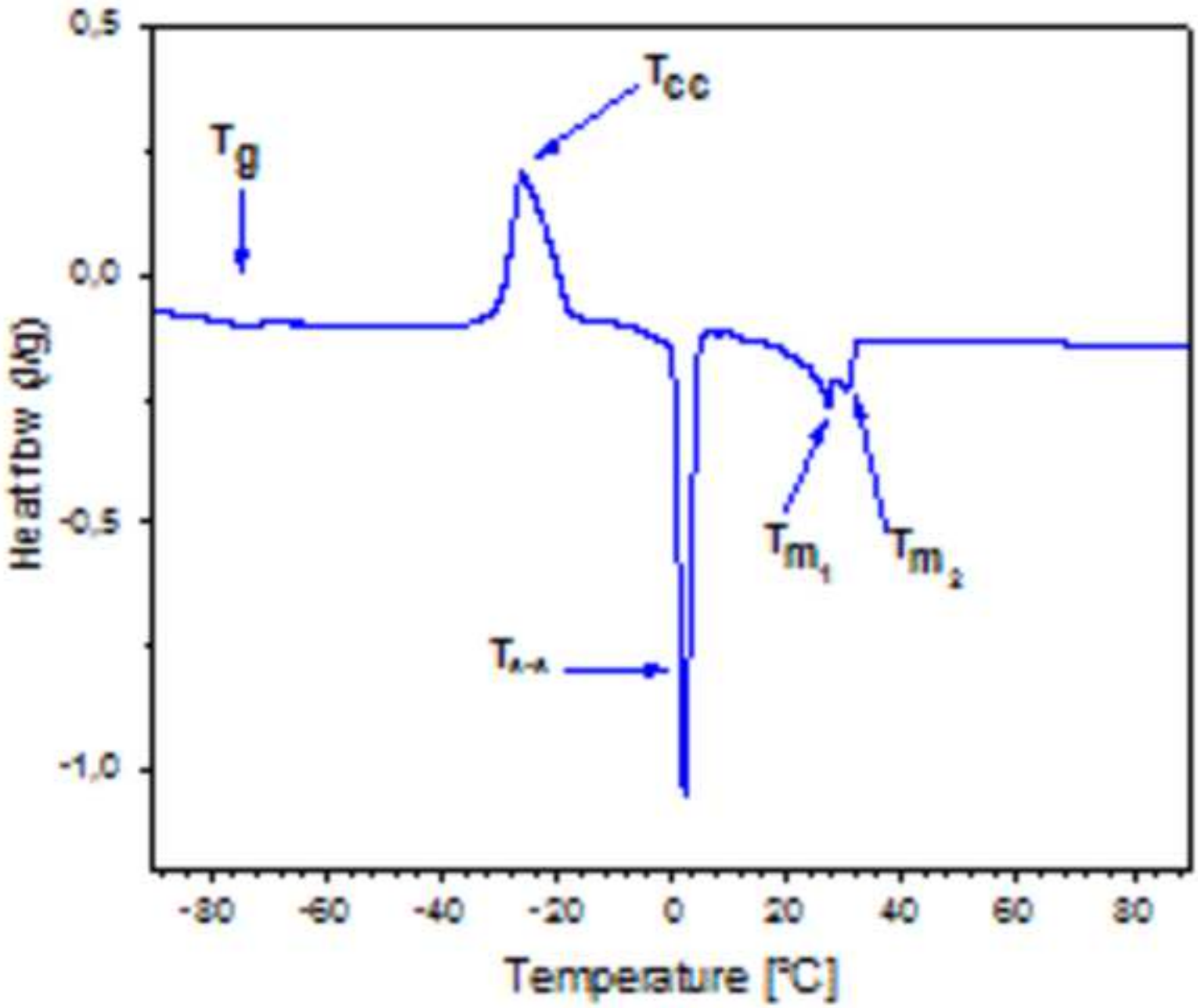

Figure(s)

Click here to access/download;Figure(s);Figure 8 TGA.tif

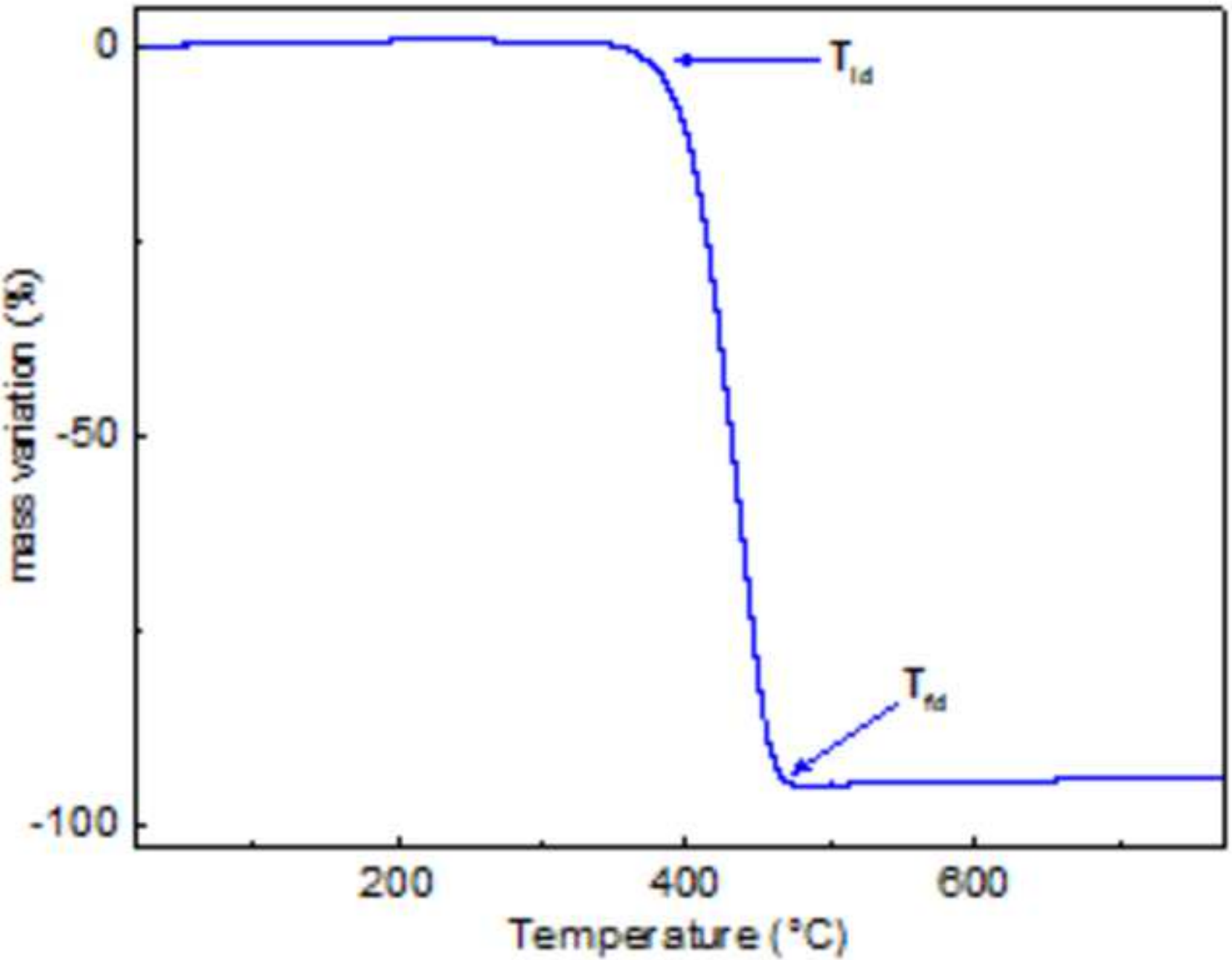

Scheme

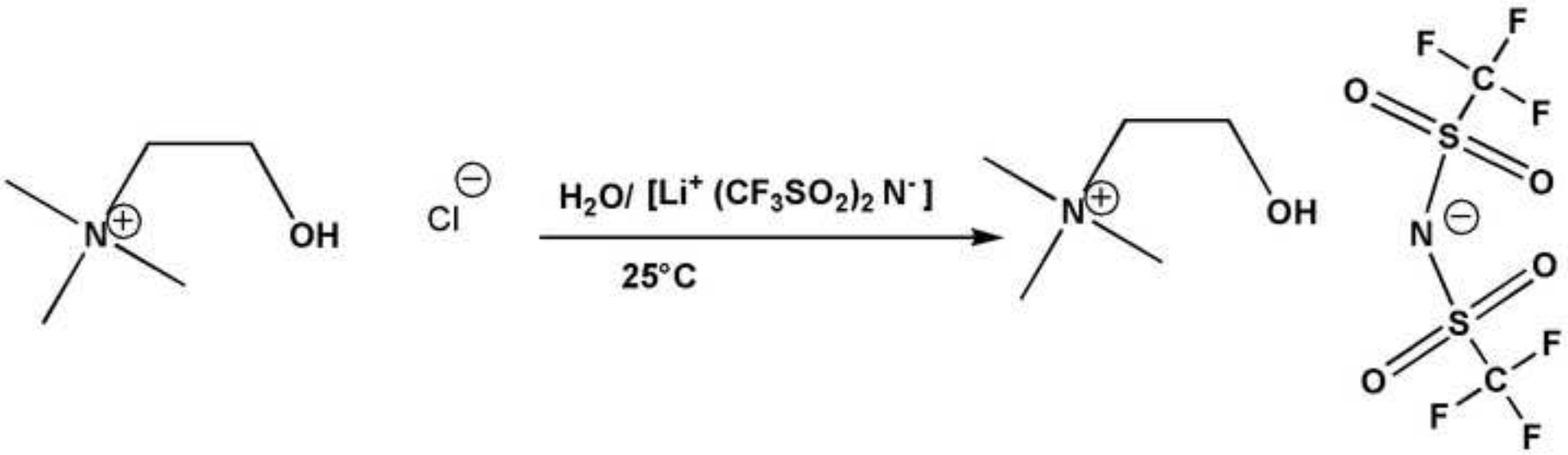

Graphical Abstract

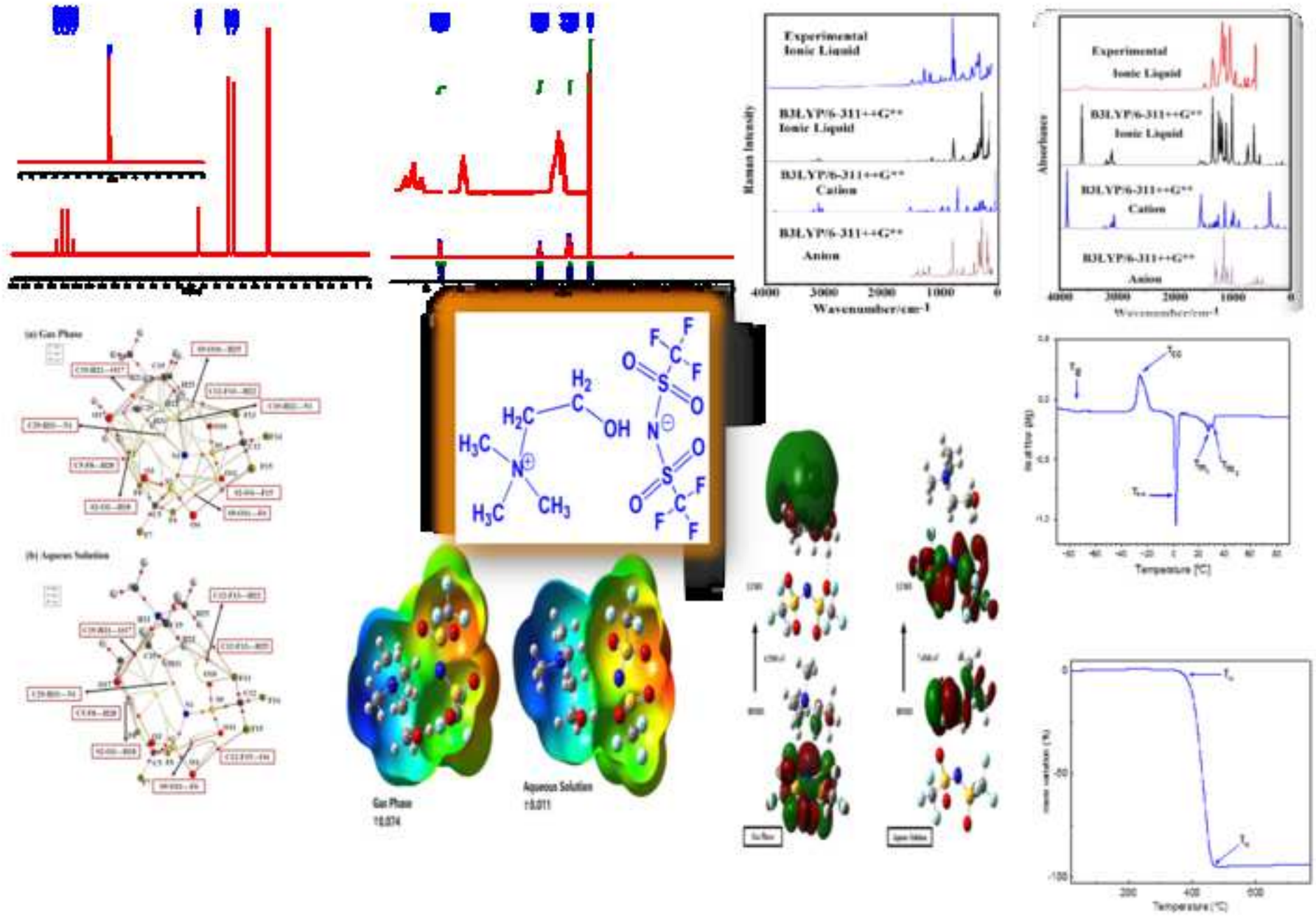

Table 1. Observed and calculated ^{1}H chemical shifts (δ in ppm) of $[CHOL^{+}][(CF_3SO_2)_2N^{-}]$ IL and its cation in aqueous solution by using the hybrid B3LYP/6-311++G**method.

Atoms	B3LYP/6-311++G**method		Exp.[a]
	$[CHOL^{+}]$	$[CHOL^{+}]NTFS_2^{-}]$[a]	
18-H	1.65	3.50	5.29
20-H	2.93	2.91	3.10
21-H	3.34	3.56	3.10
22-H	2.94	2.98	3.10
24-H	2.99	2.94	3.10
25-H	3.08	3.11	3.10
26-H	3.01	2.94	3.10
28-H	4.06	4.08	3.83
30-H	3.29	3.05	3.40
31-H	3.57	4.02	3.40
32-H	4.52	4.21	3.83
34-H	2.96	2.97	3.10
35-H	2.64	2.68	3.10
36-H	3.34	3.53	3.10
RMSD	1.01	0.57	

[a]This work.

Table 2. Observed and calculated ^{13}C chemical shifts (δ in ppm) of $[CHOL^{+}][(CF_3SO_2)_2N^{-}]$IL and its cation in gas phase by using the hybrid B3LYP/6-311++G**method

Atoms	B3LYP/6-311++G**method		Exp.[a]
	$[CHOL^{+}]$	$[CHOL^{+}]NTFS_2^{-}]$[a]	
5-C	Anion	130.34	119.23
12-C	Anion	130.34	119.23
19-C	53.71	54.36	52.92
23-C	57.67	58.01	52.92
27-C	61.97	61.94	55.15
29-C	71.34	72.62	66.84
33-C	51.09	50.69	52.92
RMSD	4.32	7.16	

[a]This work.

Table 3. Observed and calculated ^{19}F chemical shifts (δ in ppm) of $[CHOL^+][(NTFS_2^-]$ IL and its cation in gas phase by using the hybrid B3LYP method.

Atoms	B3LYP/6-311++G**method		Exp.[a]
	$[NTFS_2^-]$[b]	$[CHOL^+]NTFS_2^-]$[a]	
6-F	-108.45	-101.19	-78.97
7-F	-112.64	-102.79	-78.97
8-F	-113.82	-98.1	-78.97
13-F	-108.45	-96.85	-78.97
14-F	-112.64	-103.12	-78.97
15-F	-113.82	-100.78	-78.97
RMSD	**32.75**	**21.62**	

[a]This work.

Table 4. Calculated uncorrected and corrected by ZPVE total energies (*E* and E_{ZPVE}), dipole moments (μ) and volumes (V) of $[CHOL^+][(CF_3SO_2)_2N^-]$ ionic liquid and its cation and anion in gas phase and aqueous solution by using the B3LYP/6-311++G** method.

B3LYP/6-311++G** Method				
$[CHOL^+]$				
Species	E (Hartrees)	E_{ZPVE} (Hartrees)	μ (D)	V ($Å^3$)
Gas Phase	-328.7894	-328.5924	1.95	136.1
Aqueus Solution	-328.8820	-328.6852	3.69	137.7
$[(CF_3SO_2)_2N^-]$				
Gas Phase	-1827.6092	-1827.5572	4.36	183.1
Aqueus Solution	-1827.6810	-1827.5620	7.04	180.4
$[CHOL^+][(CF_3SO_2)_2N^-]$				
Gas Phase	-2156.5257	-2156.2746	14.22	311.5
Aqueus Solution	-2156.5699	-2156.3202	24.19	317.6

Zero point vibrational energy (ZPVE)

Table 5. Calculated distances (in Å) of interactions predicted for the[$CHOL^+$][$(CF_3SO_2)_2N^-$] ionic liquid in gas phase and aqueous solution by using the B3LYP/6-311++G** Method.

Interactions	Gas Phase	Aqueous solution
S2-O3···H18	1.832	1.948
S2-O4···F15	3.046	3.221
S9-O11···F6	3.015	3.234
S9-O10···H25	2.160	-----
C5-F8···H28	2.882	3.292
C12-F13···H22	2.790	3.098
C12-F13···H25	----	2.838
C19-H21···O17	2.283	2.508
C19-H22···N1	2.519	----
C29-H31···N1	2.224	2.664

[a]This work; Letters bold, shorter distances.

Table 6. Calculated geometrical parameters of $[CHOL^+][(CF_3SO_2)_2N^-]$ ionic liquid in gas phase and aqueous solution by using the B3LYP/6-311++G**method compared with the corresponding experimental ones [19].

Parameters	B3LYP Method 6-311++G**		Exp[b]
	$[CHOL^+][(CF_3SO_2)_2N^-]$[a]		
	Gas Phase	Solution	
Bond lengths (Å)			
N1-S2	1.621	1.608	1.620
N1-S9	1.627	1.612	1.616
S2-O3	1.473	1.469	1.475
S2-O4	1.452	1.465	1.458
S2-C5	1.897	1.892	1.870
O3-H18	1.832	1.948	1.703
C5-F6	1.327	1.334	1.333
C5-F7	1.334	1.335	1.334
C5-F8	1.349	1.334	1.343
S9-O10	1.469	1.464	1.477
S9-O11	1.453	1.466	1.457
S9-C12	1.896	1.892	1.875
C12-F13	1.348	1.334	1.345
C12-F14	1.335	1.335	1.336
C12-F15	1.328	1.334	1.332
N16-C19	1.514	1.503	1.515
N16-C23	1.508	1.504	1.508
N16-C29	1.533	1.525	1.540
N16-C33	1.497	1.502	1.501
O17-H18	0.977	0.971	0.980
O17-C27	1.409	1.428	1.406
RMSD	**0.029**	**0.055**	
Bond angles (º)			
S2-N1-S9	126.2	125.7	127.4
N1-S2-O3	105.6	107.7	103.0
N1-S2-O4	117.2	117.1	117.7
N1-S2-C5	104.5	103.4	104.5
O3-S2-O4	119.3	117.9	120.2
O3-S2-C5	102.4	103.9	103.4
O4-S2-C5	105.9	104.9	105.8
S2-O3-H18	137.4	130.0	127.8
S2-C5-F6	111.7	110.1	111.0
S2-C5-F7	109.2	109.1	110.5
S2-C5-F8	109.6	110.3	109.2
F6-C5-F7	109.4	109.1	108.8
F6-C5-F8	108.6	109.1	108.8
F7-C5-F8	108.4	109.1	108.2

N1-S9-O10	105.3	107.8	103.8
N1-S9-O11	116.9	116.6	118.0
N1-S9-C12	104.0	102.9	105.5
O10-S9-O11	120.0	118.4	119.4
O10-S9-C12	102.9	104.2	102.5
O11-S9-C12	105.8	104.9	105.5
S9-C12-F13	109.8	110.3	109.8
S9-C12-F14	109.1	109.2	109.4
S9-C12-F15	111.6	110.2	111.1
F13-C12-F14	108.3	109.0	108.4
F13-C12-F15	108.6	109.1	108.8
F14-C12-F15	109.3	109.1	109.1
C19-N16-C23	108.2	108.4	108.1
C19-N16-C29	110.9	111.8	110.5
C19-N16-C33	109.3	109.4	109.4
C23-N16-C29	107.4	107.2	107.6
C23-N16-C33	109.5	108.5	109.6
C29-N16-C33	111.5	111.3	111.2
H18-O17-C27	108.8	108.5	110.0
O17-C27-C29	114.7	115.1	118.5
N16-C29-C27	116.3	117.6	115.7
RMSD	**1.8**	**1.3**	

[a]This work, [b]From Ref [19].

Table 7. Observed and calculated wavenumbers (cm^{-1}) and assignments for $[CHOL^+][(CF_3SO_2)_2N^-]$ ionic liquid and its cation and anion in gas phase by using the hybrid B3LYP/6-311++G** Method.

Experimental[a]		B3LYP/6-311++G**					
		$[CHOL^+]$[a]		$[(CF_3SO_2)_2N^-]$[c]		$[CHOL^+][(CF_3SO_2)_2N^-]$[a]	
IR	Raman	SQM[b]	Assignments[a]	SQM[c]	Assignments[c]	SQM[b]	Assignments[a]
3555w		3672	νO2-H3			3426	νO17-H18
3068vw		3064	ν_aCH_3(C4)			3059	ν_aCH_3(C19)
		3044	ν_aCH_3(C18)			3039	ν_aCH_3(C19)
		3035	ν_aCH_3(C8)			3036	ν_aCH_3(C33)
		3032	ν_aCH_3(C8)			3021	ν_aCH_3(C33)
		3029	ν_aCH_3(C4)			3017	ν_aCH_3(C23)
	3021w	3027	ν_aCH_3(C18)			3014	ν_aCH_3(C23)
2988vw		3003	ν_aCH_2(C14)			2988	ν_aCH_2(C29)
2958vw	2965w	2953	ν_sCH_2(C14)			2946	ν_sCH_3(C19)
		2948	ν_sCH_3(C4)			2941	ν_aCH_2(C27)
		2944	ν_sCH_3(C18)			2937	ν_sCH_3(C33)
		2940	ν_sCH_3(C8)			2928	ν_sCH_2(C29)
2908vw	2917w	2921	ν_aCH_2(C12)			2921	ν_sCH_3(C23)
	2813w	2890	ν_sCH_2(C12)			2888	ν_sCH_2(C27)
1652w	1530vw	1522	δCH_2(C12)			1507	δCH_2(C27)
1497w						1500	δCH_2(C29)
1485sh		1487	δCH_2(C14)			1473	δ_aCH_3(C19)
	1463sh	1464	δ_aCH_3(C4)			1462	δ_aCH_3(C23)
	1454sh	1452	δ_aCH_3(C8) δ_aCH_3(C18)			1443	δ_aCH_3(C33)
1438w	1441w	1445	δ_aCH_3(C18)			1438	δ_aCH_3(C23)
		1431	δ_aCH_3(C4), δ_aCH_3(C18)			1433	δ_aCH_3(C33)
		1426	δ_aCH_3(C18), δ_aCH_3(C8)			1429	δ_sCH_3(C23),δ_sCH_3(C19)
	1419sh	1424	δ_aCH_3(C8)			1411	δ_aCH_3(C19)
		1414	δ_aCH_3(C4)			1398	δO5-H18-O17, δOH
1396sh		1397	$wagCH_2$(C12)			1395	$wagCH_2$(C29), δ_sCH_3(C33)
1382sh		1383	δ_sCH_3(C4)			1388	δ_sCH_3(C23),δ_sCH_3(C19)
1361s		1381	δ_sCH_3(C18), δ_sCH_3(C8)			1379	δ_sCH_3(C33)
	1350sh	1352	$wagCH_2$(C14)			1350	$wagCH_2$(C27), $wagCH_2$(C29)
1331sh	1324w	1335	ρCH_2(C14)			1325	ρCH_2(C29)
1265sh		1276	ρCH_2(C12)			1266	ρCH_2(C27)
						1261	δO5-H18-O17,τO5-H18
1240sh	1248sh	1259	$\rho'CH_3$(C18), ρCH_3(C8)	1236	ν_aSO_2 (S2)	1258	ν_aSO_2 (S3)
	1230m			1221	ν_aSO_2 (S3)	1234	ν_aSO_2 (S2)
1227sh	1215sh	1228	ρCH_3(C4),ρCH_3(C18)			1223	δO5-H18-O17, $\rho'CH_3$(C19)
1197vs		1208	$\rho'CH_3$(C8), ρCH_2(C14)			1204	δO5-H18-O17,τO5-H18
1197vs	1189w	1164	δOH			1166	ν_aCF_3(C8)
				1157	ν_aCF_3(C9)	1157	ν_aCF_3(C9)
1149s				1150	ν_sCF_3(C8)	1149	ν_aCF_3(C8), ν_sCF_3(C8)
						1139	ν_sCF_3(C8)
1134sh	1124m	1124	$\rho'CH_3$(C18)	1124	ν_aCF_3(C9)	1122	ρCH_3(C23), ρCH_3(C19)
		1112	ρCH_3(C8), $\rho'CH_3$(C4)	1120	ν_aCF_3(C8)	1116	$\rho'CH_3$(C33)
1103sh	1106sh			1108	ν_aCF_3(C9)	1107	ν_aCF_3(C9)

				1104	ν_aCF_3(C8)	1104	ν_aCF_3(C8)
1071vs	1073sh	1059	νC12-O2			1065	νC27-O17,νC27-C29
1056sh		1053	τwCH_2(C12)	1056	νsSO_2 (S2)	1058	ρ'CH_3(C23),ρ'CH_3(C19) ρCH_3(C33)
1040sh	1041w	1050	ρ'CH_3(C8), ρCH_3(C18) ρCH_3(C4)	1041	νsSO_2 (S3)	1039	δO5-H18-O17,τO5-H18
1038sh						1036	νsSO_2 (S3)
1026sh	993w					1029	νsSO_2 (S2)
972m	968sh			970	νS2-N1	960	τwCH_2(C27)
940w	948w	946	νC12-C14			940	νS2-N1, νS3-N1
		923	νN1-C8			932	νN16-C33
899sh	887sh	915	νN1-C4,νN1-C18			914	νN16-C23
885w	858w	843	τwCH_2(C14),νN1-C8			847	τwCH_2(C29)
808m		828	νN1-C14,νN1-C4			827	νN16-C19
760m	750sh	792w		732	ν_sCF_3(C9)	737	ν_sCF_3(C9)
736w	735vs			723	δ_sCF_3(C8)	729	δ_sCF_3(C8),δ_sCF_3(C9)
674m	705sh			684	νS3-N1	688	τO5-H18,τH18-O17
674m		678	νN1-C14			679	νN16-C29
649sh						644	τH18-O17
628s	626w			616	wagSO_2(S3)	590	wagSO_2(S2), wagSO_2(S3)
	581sh					582	δS2N1S3
				568	wagSO_2(S2)	559	τO5-H18,δSO_2(S2)
	550w			550	δ_aCF_3(C9)	552	δ_aCF_3(C9)
				540	δ_aCF_3(C9)	539	δ_aCF_3(C9)
	533sh			538	δ_aCF_3(C8)	535	δ_aCF_3(C8)
		528	δN1C14C12, δO2C12C14	528	δ_aCF_3(C8)	534	δN16C29C27
	515sh			497	δSO_2(S3)	515	δ_aCF_3(C8)
	509sh			483	δSO_2(S2)	496	δSO_2(S3),δSO_2(S2)
	446w	443	δC8N1C18			449	δC23N16C19
		435	δC18N1C4			440	δC33N16C19
	416sh	405	δO2C12C14	409	τ_wSO_2(S3)	414	δC23N16C33, δO17C27C29
	398m					369	τ_wSO_2(S2),τ_wSO_2(S3),ρCF_3(C8)
		363	ρ'N1-C14, δC8N1C4	366	τ_wSO_2(S2)	365	ρ'N16-C29
	354sh					358	δS2-O5-H18
	346sh			331	ρSO_2(S3)	344	δN1S3C9,δN1S2C8
	333sh			310	ρCF_3(C9)	326	δS2-O5-H18
	314m	301	ρN1-C14	303	ρCF_3(C8)	301	ρN16-C29
		293	τOH			293	δS2O5H18,ρSO_2(S2)
						290	δO5H18O17,τO5-H18
	280sh					289	τO5-H18,δS2-O5-H18
	275s	282	τ_wCH_3(C18)			274	τ_wCH_3(C23)
				284	ρSO_2(S2)	274	ρSO_2(S2),ρSO_2(S3)
	257sh	259	τ_wCH_3(C4),τ_wCH_3(C8)	259	νS3-C9	255	τO5-H18τH18-O17
	242sh	250	δN1C14C12	252	νS2-C8	250	νS2-C8,ρ'CF_3(C8), νS3-C9 ρ'CF_3(C9)
		210	τ_wCH_3(C4),τ_wCH_3(C8)			218	τ_wCH_3(C33) τ_wCH_3(C19)
	211sh					207	δN1S3C9,δN1S2C8
	192sh			187	ρ'CF_3(C9)	191	τO5-H18,τH18-O17
				186	ρ'CF_3(C8)	189	ρCF_3(C9)
	168w	162	τC12-C14	163	δN1S3C9	173	τO5-H18,τH18-O17

155sh			149	δN1S2C8	154	τO5-H18,τH18-O17
133sh					136	νO5-H18
118m					112	τO5-H18,τH18-O17
105sh			100	δS2N1S3	103	δN1S3C9,δN1S2C8
83sh					82	τO5-H18, δO5H18O17
70sh					65	τwC29-N16,τC27-C29
50m	57	τwC14-N1	60	τS2-N1	54	τS2-N1,τS3-N1
					41	δS2O5H18,δO5H18O17
			38	$\tau_w CF_3$(C9)	37	δS2O5H18,τOH,$\tau_w CF_3$(C8) $\tau_w CF_3$(C9)
			30	$\tau_w CF_3$(C8)	28	δS2O5H18, τO5-H18
					23	τwO5-S2
					19	τO5-H18, τH18-O17
			5	τS3-N1	15	τO5-H18

Abbreviations: ν, stretching;β, deformation in the plane; γ,deformation out of plane; wag, wagging;τ , torsion;ρ,rocking;τw,twisting;δ,deformation; a, antisymmetric; s, symmetric; [a]This work, [b]From scaled quantum mechanics force field with B3LYP/6-311++G** method, [b]From scaled quantum mechanics force field with B3LYP/6-311++G** method from Ref [22].

Table 8. Scaled internal force constants for the [$CHOL^+$][$(CF_3SO_2)_2N^-$]ionic liquid and its cation and anion in gas phase and aqueous solution by using the hybrid B3LYP/6-311++G**method.

Force constants	B3LYP method				
	6-311++G**				
	[$CHOL^+$][a]		[$(CF_3SO_2)_2N^-$][b]	[$CHOL^+$][$(CF_3SO_2)_2N^-$][a]	
	Gas	Aqueous Solution	Gas	Gas	Aqueous Solution
f(νOH)	7.54	7.41		7.13	7.17
f(νC-O)	4.96	4.52		5.19	4.66
f(νN-C)	3.76	3.90		3.82	3.91
f(νCH₂)	4.77	4.83		4.75	4.86
f(νCH₃)	4.98	5,00		4.96	5.01
f(δCH₂)	0.87	0.83		0.88	0.83
f(δCH₃)	0.55	0.54		0.55	0.54
f(δOH)	0.67	0.67		1.96	0.92
f(νSO₂)			8.20	8.36	7.91
f(νCF₃)			5.31	5.49	5.43
f(νN-S)			4.56	4.17	4.43
f(νS-C)			2.17	2.17	2.25
f(δSO₂)			1.90	1.93	1.82
f(δCF₃)			1.51	1.49	1.44

Units are mdyn $Å^{-1}$ for stretching and mdyn Å rad^{-2} for angle deformations. [a]This work, [b]From Ref [22].

MATERIAL SUPPORTING TO

Synthesis, NMR, FT-IR, FT-Raman spectra and thermal studies of Choline bis(trifluoromethylsulfonyl)imide Ionic Liquid combined with DFT Calculations.

Boumediene Haddad[1,2,*], Silvia Antonia Brandán[3],María V. Castillo[3], Touil Aya Khadidja[1,4], Annalisa Paolone[5], Bekhaled Fetouhi[6,7],Nathalie Bar[2],Didier Villemin[2], Mustapha Rahmouni[7], Serge Bresson[8]

[1]Department of Chemistry, Faculty of Sciences, University of Saida - Dr. Moulay-Tahar, 20000, Algeria.
[2] LCMT, ENSICAEN, UMR 6507 CNRS, University of Caen, 6 bd MlJuin, 14050 Caen, France
[3]Cátedra de Química General, Instituto de Química Inorgánica, Facultad de Bioquímica. Química y Farmacia, Universidad Nacional de Tucumán, Ayacucho 471, (4000) San Miguel de Tucumán, Tucumán, Argentina
[4]Chemistry Laboratory of Synthesis, Properties, and Applications (CLSPA-Saida), University of Saida, Algeria
[5]CNR-ISC, U.O.S. La Sapienza, Piazzale A. Moro 5, 00185 Roma, Italy
[6]Faculty of Natural and Life Sciences, University of Tiaret, BP78 ZaarouraTiaret 14000, Algeria
[7] Synthesis and Catalysis Laboratory LSCT, Tiaret University, Tiaret, Algeria
[8]UP Transformations & Agro-Ressources, Institut Polytechnique UniLaSalle, SFR Condorcet 3417, BP 30313, F-60026 Beauvais, France.

*Corresponding author: Tel.: +213676802567
E-mail :haddadboumediene@yahoo.com (HADDAD Boumediene).

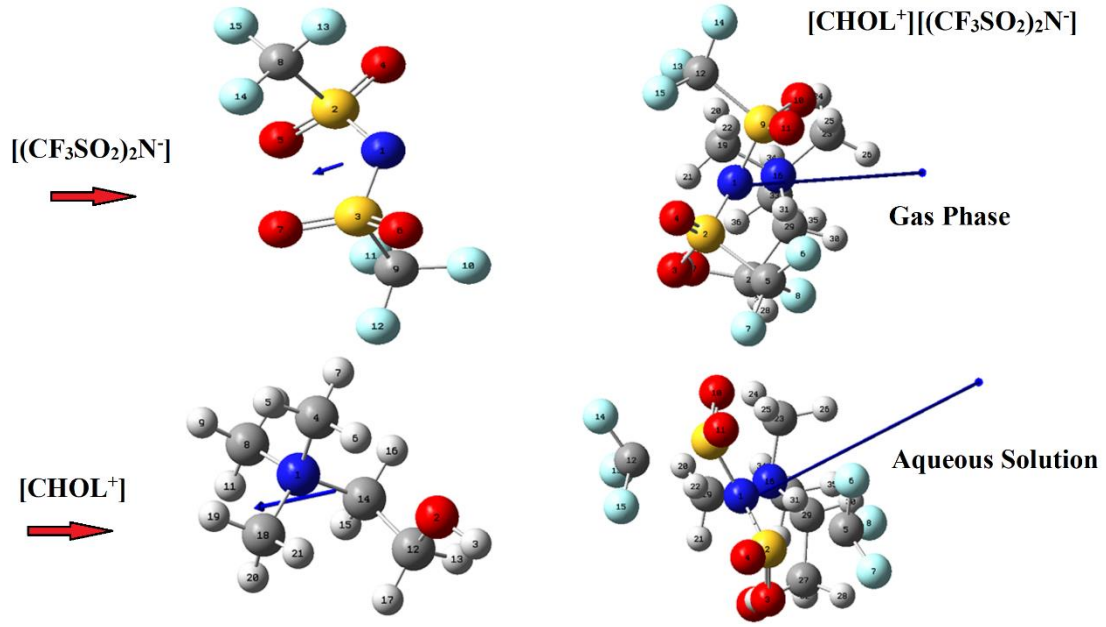

Figure S1. Orientations and directions of dipole moment vectors for $[CHOL^+][(CF_3SO_2)_2N^-]$ IL in both media and its $[CHOL^+]$ cationand $[(CF_3SO_2)_2N^-]$anion in gas phase by using the hybrid B3LYP/6-311++G**level of theory.

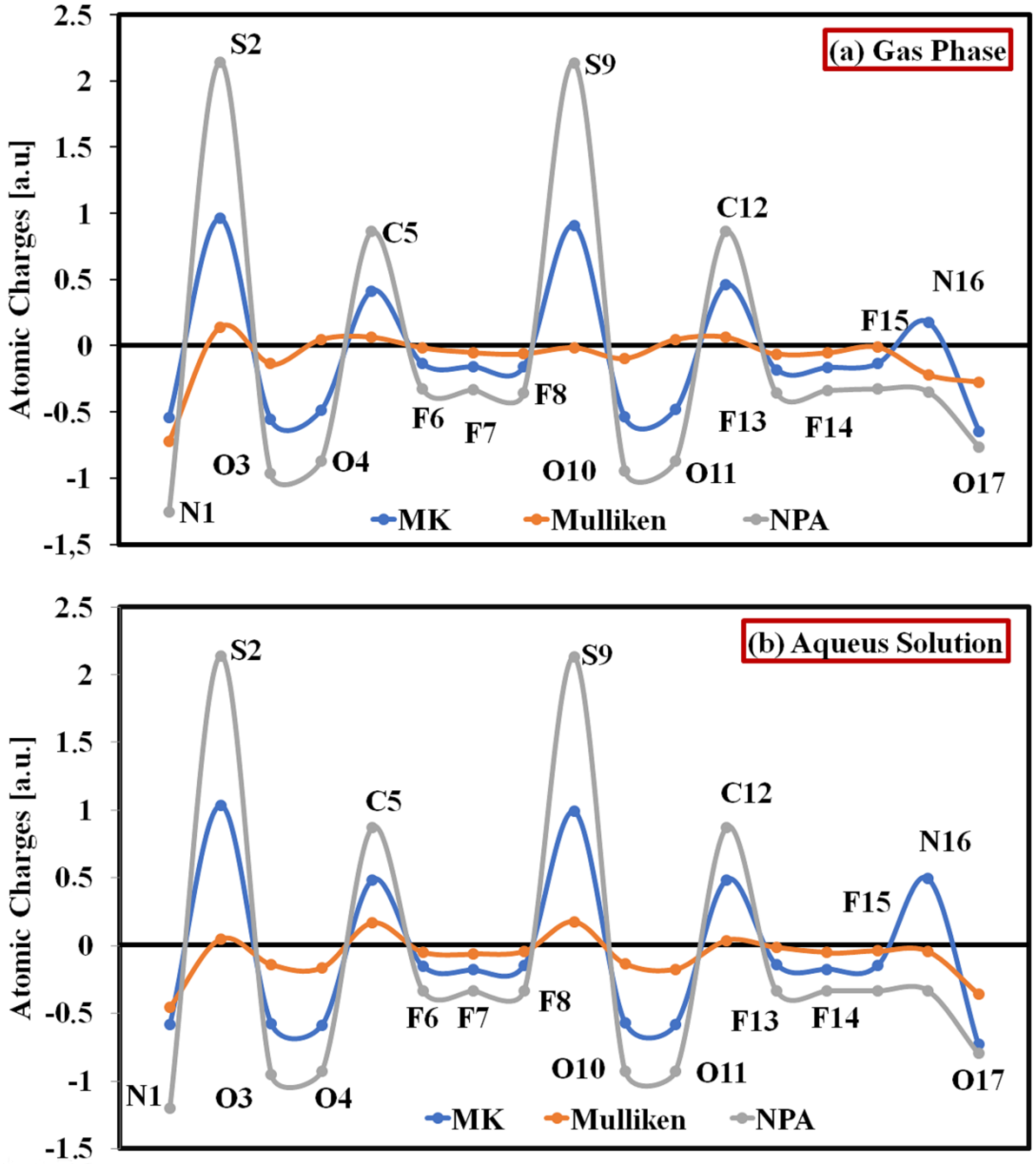

Figure S2. Calculated atomic MK, Mulliken and NPA charges on the N, C, and F atoms of $[CHOL^+][(CF_3SO_2)_2N^-]$ IL, (a) in gas phase and (b) in aqueous solution by using the B3LYP/6-311++G** level of theory.

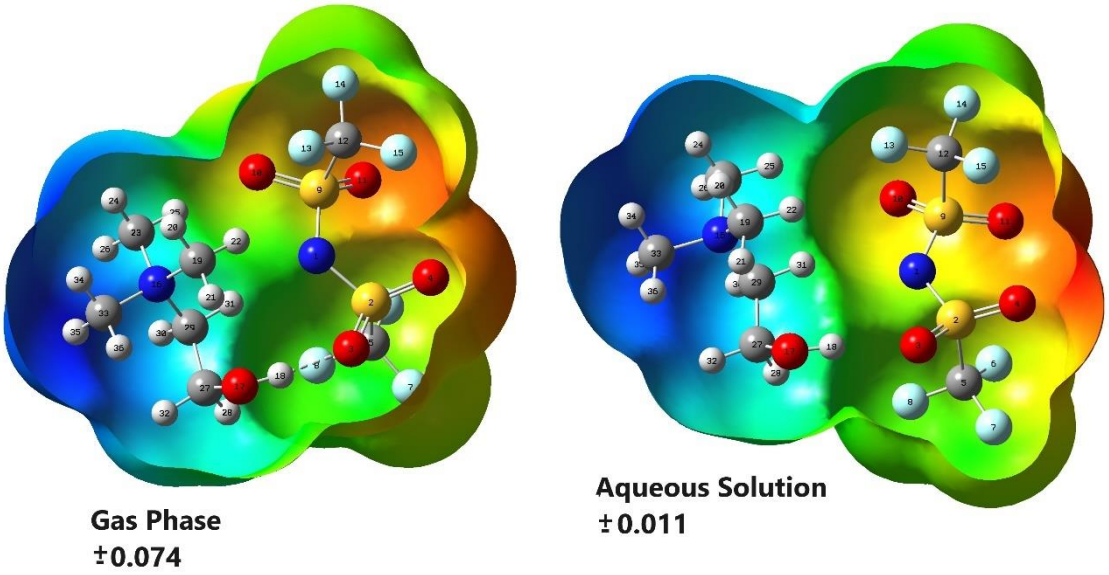

Figure S3. Calculated electrostatic potential surfaces on the molecular surface of[$CHOL^+$][$(CF_3SO_2)_2N^-$] IL in gas phase and in aqueous solution by using the B3LYP/6-311++G** level of theory.Isodensity value of 0.004.

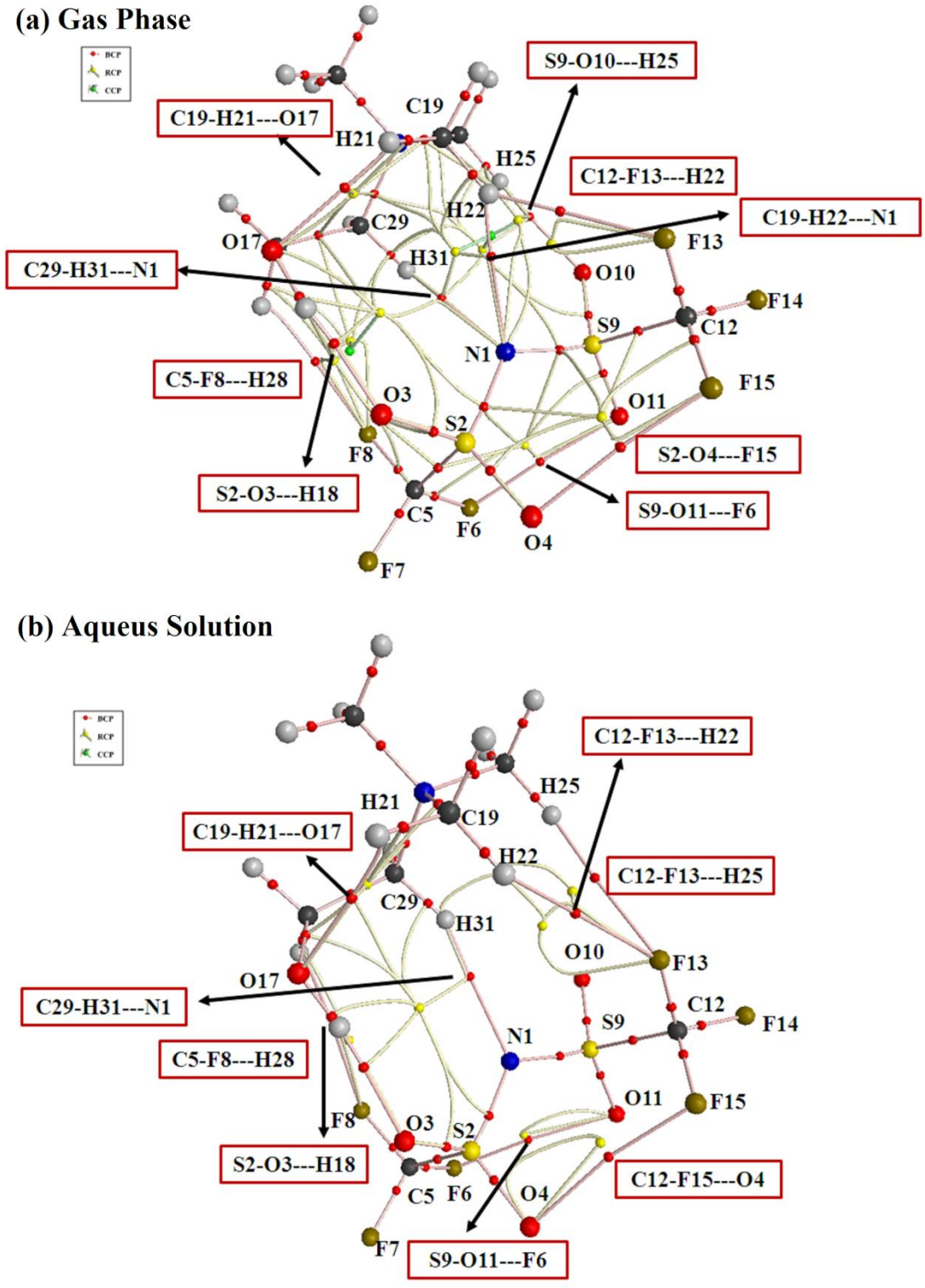

Figure S4. Molecular graphicsfor [$CHOL^+$][$(CF_3SO_2)_2N^-$] IL,(a) in gas phase and (b) in aqueous solution by using the B3LYP/6-311++G** level of theory.

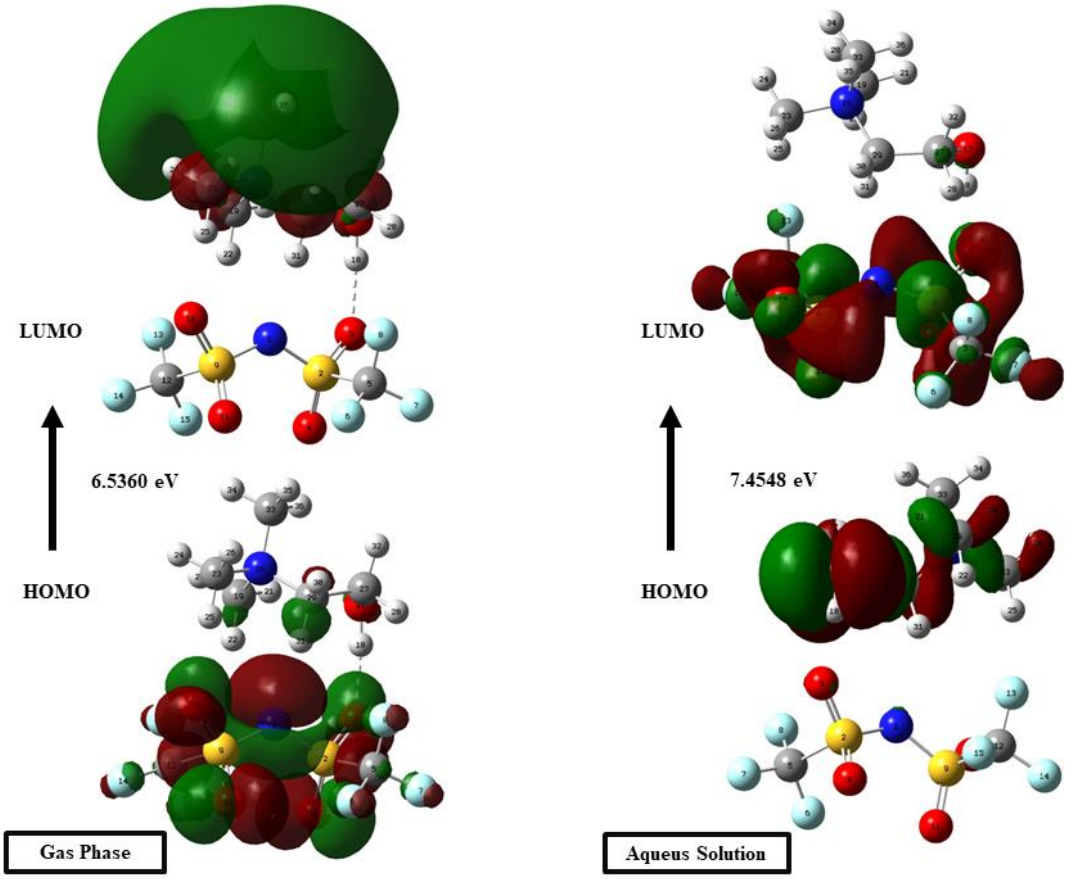

Figure S5. Characteristics of HOMO-LUMO orbitals for [CHOL$^+$] [$(CF_3SO_2)_2N^-$] IL showing the gap values in gas phase and aqueous solution by using the B3LYP/6-311++G** level of theory.

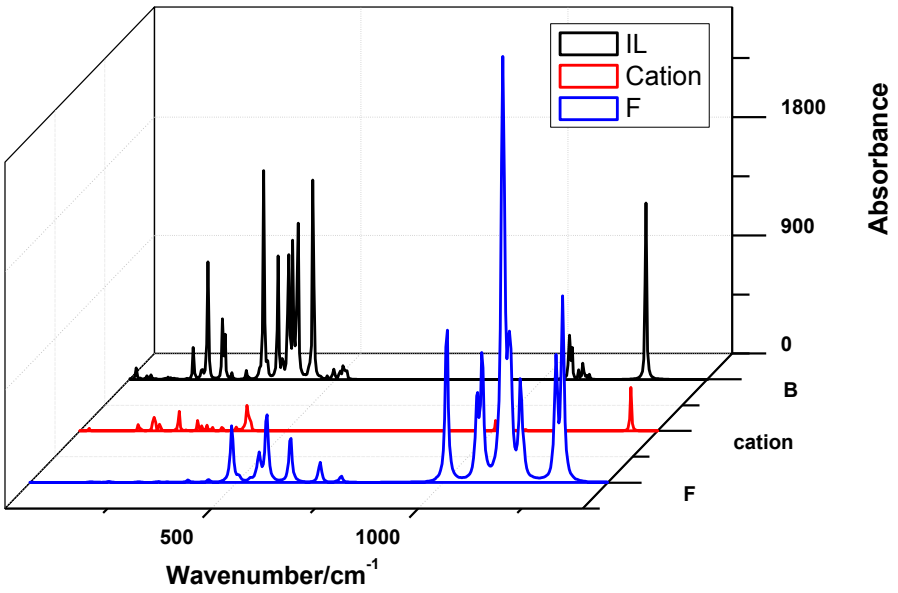

Figure S6. Theoretical FT-IR spectrum of ionic liquid in the gas phase (black colour) compared with the corresponding predicted for the cation (red colour) and anion(blue colour) by using the B3LYP/6-311++G** level of theory.

Table S1. Calculated atomic MK, Mulliken and NPA charges on the atoms of[$CHOL^+$][$(CF_3SO_2)_2N^-$] IL in gas phase and in aqueous solution by using the B3LYP/6-311++G** level of theory.

B3LYP/6-311G**METHOD						
[$CHOL^+$][$(CF_3SO_2)_2N^-$]						
Atoms	Gas Phase			AqueousSolution		
	MK	Mulliken	NPA	MK	Mulliken	NPA
1 N	-0.540	-0.722	-1.254	-0.589	-0.457	-1.206
2 S	0.961	0.139	2.140	1.031	0.047	2.134
3 O	-0.556	-0.134	-0.961	-0.583	-0.144	-0.954
4 O	-0.485	0.049	-0.868	-0.595	-0.168	-0.931
5 C	0.414	0.063	0.862	0.483	0.166	0.871
6 F	-0.132	-0.016	-0.325	-0.154	-0.050	-0.338
7 F	-0.157	-0.051	-0.334	-0.182	-0.067	-0.337
8 F	-0.158	-0.061	-0.359	-0.148	-0.046	-0.336
9 S	0.908	-0.014	2.132	0.987	0.174	2.128
10 O	-0.539	-0.095	-0.943	-0.576	-0.136	-0.935
11 O	-0.478	0.049	-0.872	-0.588	-0.178	-0.935
12 C	0.460	0.067	0.861	0.483	0.034	0.869
13 F	-0.182	-0.064	-0.356	-0.146	-0.018	-0.335
14 F	-0.167	-0.055	-0.336	-0.178	-0.054	-0.337
15 F	-0.135	-0.011	-0.326	-0.152	-0.041	-0.339
16 N	0.177	-0.218	-0.348	0.493	-0.045	-0.339
17 O	-0.647	-0.273	-0.765	-0.731	-0.365	-0.797
18 H	0.463	0.392	0.509	0.462	0.416	0.501
19 C	-0.278	-0.493	-0.359	-0.450	-0.414	-0.352
20 H	0.150	0.182	0.199	0.184	0.234	0.224
21 H	0.177	0.244	0.243	0.205	0.222	0.231
22 H	0.125	0.249	0.248	0.194	0.231	0.227
23 C	-0.382	-0.228	-0.358	-0.412	-0.306	-0.350
24 H	0.172	0.179	0.207	0.191	0.212	0.228
25 H	0.222	0.325	0.268	0.161	0.227	0.228
26 H	0.172	0.181	0.205	0.186	0.214	0.227
27 C	0.161	-0.619	-0.048	0.110	-0.630	-0.053
28 H	0.055	0.219	0.195	0.076	0.242	0.196
29 C	-0.202	-0.422	-0.201	-0.204	-0.388	-0.192
30 H	0.133	0.166	0.207	0.153	0.222	0.237
31 H	0.102	0.504	0.262	0.090	0.380	0.238
32 H	0.068	0.160	0.171	0.111	0.198	0.198
33 C	-0.594	-0.296	-0.350	-0.647	-0.360	-0.355
34 H	0.218	0.182	0.214	0.234	0.210	0.229
35 H	0.223	0.204	0.212	0.232	0.228	0.228
36 H	0.268	0.219	0.228	0.270	0.210	0.228

Table S2. Molecular electrostatic potentials (MEP) and Bond orders (BO) expressed as Wiberg bond index, totals by atom for the[$CHOL^+$][$(CF_3SO_2)_2N^-$] IL in gas phase and in aqueous solution by using the B3LYP/6-311++G** level of theory.

Atoms	MEP (a.u.)		Bond Orders	
	Gas	AqueousSolution	Gas	AqueousSolution
1 N	-18.393	-18.401	2.476	2.531
2 S	-59.004	-59.027	4.280	4.280
3 O	-22.369	-22.388	1.605	1.609
4 O	-22.375	-22.430	1.723	1.634
5 C	-14.493	-14.508	3.645	3.655
6 F	-26.551	-26.576	1.074	1.057
7 F	-26.550	-26.569	1.058	1.054
8 F	-26.547	-26.550	1.026	1.059
9 S	-59.007	-59.030	4.286	4.287
10 O	-22.373	-22.402	1.620	1.624
11 O	-22.376	-22.433	1.718	1.629
12 C	-14.494	-14.496	3.644	3.655
13 F	-26.548	-26.524	1.028	1.058
14 F	-26.551	-26.559	1.056	1.053
15 F	-26.552	-26.565	1.073	1.057
16 N	-18.222	-18.174	3.567	3.570
17 O	-22.353	-22.359	1.793	1.751
18 H	-0.991	-1.001	0.745	0.753
19 C	-14.696	-14.653	3.740	3.758
20 H	-1.051	-1.000	0.962	0.951
21 H	-1.059	-1.031	0.943	0.949
22 H	-1.060	-1.024	0.945	0.951
23 C	-14.686	-14.638	3.750	3.755
24 H	-1.043	-0.990	0.959	0.950
25 H	-1.052	-1.015	0.930	0.950
26 H	-1.043	-0.996	0.959	0.950
27 C	-14.684	-14.665	3.865	3.838
28 H	-1.080	-1.065	0.965	0.964
29 C	-14.688	-14.650	3.803	3.820
30 H	-1.049	-1.005	0.959	0.946
31 H	-1.062	-1.038	0.941	0.947
32 H	-1.080	-1.044	0.974	0.964
33 C	-14.670	-14.627	3.784	3.759
34 H	-1.030	-0.982	0.956	0.949
35 H	-1.030	-0.983	0.957	0.949
36 H	-1.034	-0.993	0.950	0.950

Table S3. Main delocalization energy (in kJ/mol) of[$CHOL^+$][$(CF_3SO_2)_2N^-$] IL in gas phase and in aqueous solution by using the B3LYP/6-311++G** level of theory.

B3LYP/6-311G**METHOD		
[$CHOL^+$][$(CF_3SO_2)_2N^-$]		
Delocalization	Gas	PCM
LP(2)N1 →σ S2-C5*	69.1	73.3
LP(2)N1→σ S9-C12*	67.2	70.7
LP(2)O3→σ N1-S2*	67.0	72.1
LP(3)O3→σ S2-O4*	67.8	66.2
LP(3)O3→σ S2-C5*	53.2	60.2
LP(2)O4→σ N1-S2*	101.7	94.4
LP(3)O4→σ S2-O3*	72.1	60.2
LP(3)O4→σ S2-C5*	76.2	74.7
LP(2)F6→σ S2-C5*	44.4	42.3
LP(3)F6→σ C5-F8*	58.2	
LP(3)F6→σ C5-F7*		54.0
LP(2)F7→σ C5-F6*	41.8	
*LP(2)F7→σ*S2-C5*		42.1
LP(3)F7→σ C5-F6*		47.7
LP(3)F7→σ C5-F8*	63.2	42.1
LP(3)F7→σ C5-F7*	55.1	
*LP(2)F8→σ*S2-C5*		44.8
LP(3)F8→σ C5-F6*		43.1
LP(3)F8→σ C5-F7*		47.2
LP(2)O10→σ N1-S9*	72.9	77.5
LP(3)O10→σ S9-O11*	64.5	63.7
LP(3)O10→σ S9-C12*	63.2	68.5
LP(2)O11→σ N1-S9*	103.9	94.8
LP(3)O11→σ S9-O10*	67.5	54.3
LP(3)O11→σ S9-C12*	81.4	79.0
*LP(2)F13→σ*C12-F15*	46.7	
*LP(2)F13→σ*S9-C12*		44.4
*LP(3)F13→σ*C12-F14*	57.3	47.3
*LP(3)F13→σ*C12-F15*		42.9
*LP(2)F14→σ*S9-C12*		41.8
LP(3)F14→σ C12-F13*	62.0	42.8
LP(3)F14→σ C12-F15*		47
LP(2)F15→σ S 9-C12*	45.2	41.8
LP(3)F15→σ C12-F13*	54.7	
LP(3)F15→σ C12-F14*		55.0
***ΔET*$_{LP→σ^*}$**	**1556.4**	**1735.8**
*σ*S2-O3→σ*S2-O4*	87.2	214.3
*σ*S9-O10→σ*S9-O11*	118.3	
***ΔET*$_{σ^*→σ^*}$**	**205.5**	**214.3**
***ΔET*$_{TOTAL}$**	**1762.0**	**1950.1**

Table S4. Predicted intramolecular interactions for the[$CHOL^+$][$(CF_3SO_2)_2N^-$] ionic liquid in gas phase and aqueous solution by using the topological properties and the B3LYP/6-311G** Method.

Interactions[a]	
Gas Phase	Aqueous solution
S2-O3⋯H18	S2-O3⋯H18
S2-O4⋯F15	S2-O4⋯F15
S9-O11⋯F6	S9-O11⋯F6
S9-O10⋯H25	
C5-F8⋯H28	C5-F8⋯H28
C12-F13⋯H22	C12-F13⋯H22
	C12-F13⋯H25
C19-H21⋯O17	C19-H21⋯O17
C19-H22⋯N1	
C29-H31⋯N1	C29-H31⋯N1

[a]This work; Letters bold, shorter distances.

Table S5. Analysis of the topological properties for the $[CHOL^+][(CF_3SO_2)_2N^-]$ ionic liquid in gas phase and aqueous solution by using the B3LYP/6-311++G** Method.

Parameter (a.u.)	Gas Phase						
	S2-O3⋯H18	**S2-O4⋯F15**	**S9-O11⋯F6**	**C5-F8⋯H28**	**C12-F13⋯H22**	**C19-H21⋯O17**	**C29-H31⋯N1**
$\rho(r_c)$	0.0296	0.0063	0.0067	0.0032	0.0052	0.0162	0.0181
$\nabla^2\rho(r_c)$	0.1128	0.0251	0.0265	0.0142	0.0208	0.0537	0.0561
λ_1	-0.0432	-0.0051	-0.0056	-0.0028	-0.0048	-0.0172	-0.0205
λ_2	-0.0418	-0.0050	-0.0054	-0.0023	-0.0041	-0.0150	-0.0188
λ_3	0.1978	0.0352	0.0375	0.0193	0.0296	0.0859	0.0954
$\lvert\lambda_1\rvert/\lambda_3$	0.2184	0.1451	0.1483	0.1437	0.1608	0.2004	0.2146
Distance (Å)	1.821	2989	2.951	2.585	2.593	2.193	2.224
Parameter (a.u.)	Aqueussolution						
	S2-O3⋯H18	**S2-O4⋯F15**	**S9-O11⋯F6**	**C5-F8⋯H28**	**C12-F13⋯H22**	**C19-H21⋯O17**	**C29-H31⋯N1**
$\rho(r_c)$	0.0217	0.0048	0.0047	0.0012	0.0018	0.0114	0.0079
$\nabla^2\rho(r_c)$	0.0874	0.0200	0.0197	0.0060	0.0087	0.0378	0.0235
λ_1	-0.0292	-0.0033	-0.0032	-0.0009	-0.0015	-0.0106	-0.0072
λ_2	-0.0275	-0.0020	-0.0017	-0.0008	-0.0012	-0.0086	-0.0067
λ_3	0.1441	0.0253	0.0246	0.0077	0.0114	0.0570	0.0374
$\lvert\lambda_1\rvert/\lambda_3$	0.2028	0.1294	0.1283	0.1196	0.1291	0.1860	0.1918
Distance (Å)	1.955	3.210	3.223	3.274	3.043	2.482	2.622

Table S6. Analysis of the topological properties for the $[CHOL^+][(CF_3SO_2)_2N^-]$ ionic liquid in gas phase and aqueous solution by using the B3LYP/6-311++G** Method.

Parameter (a.u.)	Gas Phase		
	S9-O10⋯H25	**C19-H22⋯N1**	**C12-F13⋯H25**
$\rho(r_c)$	0.0160	0.0104	-----
$\nabla^2\rho(r_c)$	0.0576	0.0306	-----
λ_1	-0.0183	-0.0097	-----
λ_2	-0.0174	-0.0086	-----
λ_3	0.0933	0.0490	-----
$\lvert\lambda_1\rvert/\lambda_3$	0.1957	0.1988	-----
Distance (Å)	2.215	2.678	
Parameter (a.u.)	Aqueussolution		
	S9-O10⋯H25	**C19-H22⋯N1**	**C12-F13⋯H25**
$\rho(r_c)$	-----	-----	0.0030
$\nabla^2\rho(r_c)$	-----	-----	0.0132
λ_1	-----	-----	-0.0027
λ_2	-----	-----	-0.0026
λ_3	-----	-----	0.0185
$\lvert\lambda_1\rvert/\lambda_3$	-----	-----	0.1464
Distance (Å)			2.838

Table S7. Calculated HOMO and LUMO orbitals, energy band gap, global hardness (η), global softness (S) and global electrophilicity index (ω) for the $[CHOL^+][(CF_3SO_2)_2N^-]$ ionic liquid in gas phase and aqueous solution by using the B3LYP/6-311++G** method. The parameters for cation and anion in gas phase are also presented by using the B3LYP/6-311++G** method.

Frontierorbitals (eV)	Gas Phase		6-311++G**	
	6-311++G**	6-311++G**	$[CHOL^+][(CF_3SO_2)_2N^-]$[a]	
	$[CHOL^+]$	$[(CF_3SO_2)_2N^-$	Gas Phase	AqueousSolution
HOMO	-12.1197	-6.0443	-7.8229	-7.8824
LUMO	-4.0861	-1.8039	-1.2869	-0.4184
|GAP|	8.0337	4.2404	6.5360	7.4640
		Descriptors		
X	8.1029	3.9241	4.5549	4.1504
μ	-8.1029	-3.9241	-4.5549	-4.1504
η	4.0168	2.1202	3.2680	3.7320
S	0.1245	0.2358	0.1530	0.1340
ω	8.1727	3.6314	3.1743	2.3079